# SIRT2 deacetylates GRASP55 to facilitate post-mitotic Golgi assembly

Xiaoyan Zhang[1,3], Andreas Brachner[2], Eva Kukolj[2], Dea Slade[2,*], Yanzhuang Wang[1,*]

[1] Department of Molecular, Cellular and Developmental Biology, University of Michigan, 4110 Biological Sciences Building, 1105 North University Avenue, Ann Arbor MI 48109-1085, USA.
[2] Department of Biochemistry, Max Perutz Labs, University of Vienna, Vienna Biocenter, Dr. Bohr-Gasse 9, 1030 Vienna, Austria.
[3] Present address: Bio-Medical Center, College of Life Science and Technology, Huazhong Agricultural University, Wuhan, Hubei, 430070, China.

[*]Correspondence: dea.slade@univie.ac.at (D.S.) or yzwang@umich.edu (Y.W.)

Keywords: SIRT2, Golgi, acetylation, GRASP55, Golgi assembly, cell cycle

**Summary**

GRASP55 is highly acetylated on lysine-50 in mitosis and its deacetylation by SIRT2 at mitotic exit promotes Golgi assembly through facilitating GRASP55 self-interaction.

**Abstract**

Sirtuin 2 (SIRT2) is an NAD-dependent sirtuin deacetylase that regulates microtubule and chromatin dynamics, gene expression, cell cycle progression as well as nuclear envelope reassembly. Recent proteomic analyses have identified Golgi proteins as SIRT2 interactors, indicating that SIRT2 may also play a role in Golgi structure formation. Here we show that SIRT2 depletion causes Golgi fragmentation and impairs Golgi reassembly at the end of mitosis. SIRT2 interacts with the Golgi reassembly stacking protein GRASP55 in mitosis when GRASP55 is highly acetylated on K50. Expression of wild-type and the K50R acetylation-deficient mutant of GRASP55, but not the K50Q acetylation-mimetic mutant, in GRASP55 and GRASP65 double knockout cells, rescued the Golgi structure and post-mitotic Golgi reassembly. Acetylation-deficient GRASP55 exhibited a higher self-interaction efficiency, a property required for Golgi structure formation. These results demonstrate that SIRT2 regulates Golgi structure by modulating GRASP55 acetylation levels.

## Introduction

Sirtuin 2 (SIRT2) is a canonical NAD-dependent sirtuin deacetylase located in the endoplasmic reticulum (ER)-Golgi intermediate compartment (ERGIC) (Budayeva and Cristea, 2016). SIRT2 traffics between ER and Golgi, shuttles between the cytoplasm and the nucleus, and associates with the centrosomes and the mitotic spindle during metaphase (Budayeva and Cristea, 2016; Inoue et al., 2007; North and Verdin, 2007). Accordingly, known SIRT2 substrates range from microtubule, membrane trafficking and metabolic proteins to chromatin-bound proteins and mitotic regulators.

SIRT2 deacetylates alpha-tubulin and impairs cell motility and neurite outgrowth (Janke, 2014; North et al., 2003; Pandithage et al., 2008). SIRT2 has thus been implicated in neurodegenerative diseases and its inhibition has neuroprotective effects in Parkinson's and Alzheimer's disease models (Chen et al., 2015; Godena et al., 2014; Harting and Knoll, 2010; Outeiro et al., 2007; Silva et al., 2016). Furthermore, SIRT2 regulates cell survival via deacetylation of transcription factors FOXO1, NF-κB and p53 (Jin et al., 2008; Jing et al., 2007; Rothgiesser et al., 2010), which may contribute to its tumor suppressive effect found in mammary tumors, hepatocellular carcinoma and skin squamous cell carcinoma (Bosch-Presegue and Vaquero, 2011; Kim et al., 2011; Serrano et al., 2013). SIRT2 may also exert its tumor-suppressive function by ensuring normal mitotic progression via activation of the anaphase-promoting complex (Kim et al., 2011) and by destabilizing ATP-citrate lyase (Lin et al., 2013) and phosphoglycerate mutase (Tsusaka et al., 2014). Finally, SIRT2 counteracts replication stress and preserves genomic integrity by deacetylating histone H4K16 at the G2/M transition (Vaquero et al., 2006), stimulating H4K20 monomethylation (Serrano et al., 2013) as well as CDK9 (Zhang et al., 2013) and ATRIP activity (Zhang et al., 2016).

SIRT2 interactomes from MRC5 and HEK293 cells pointed to a new connection between SIRT2 and the ER-Golgi trafficking pathway (Budayeva and Cristea, 2016). Consistently, our proteomic study revealed ER and Golgi proteins as SIRT2 interacting partners (Kaufmann et al., 2016), indicating a role for SIRT2 in ER and Golgi structure formation. To date, the regulation of Golgi structural proteins by acetylation has not been reported. The Golgi apparatus is a membranous organelle that mediates protein and lipid trafficking. It has been estimated that proteins encoded by over one-third of the genes in the human genome travel through the Golgi to their final destinations. Most of these proteins are also modified by Golgi-localized enzymes. A unique structure of the Golgi is a stack of flattened cisternal membranes. Formation of the Golgi stacked structure requires two Golgi reassembly stacking proteins, GRASP55 and GRASP65, which form *trans*-oligomers to hold Golgi membranes into stacks (Shorter et al., 1999; Zhang and Wang, 2015; Zhang and Wang, 2016). Both GRASP55 and GRASP65 are peripheral membrane proteins located in the *medial/trans- and cis-*

Golgi, respectively. GRASP55 and GRASP65 self-interact to form *trans*-oligomers (Wang et al., 2003; Xiang and Wang, 2010); this property is believed to be essential for their roles in Golgi cisternal stacking (Shorter et al., 1999; Tang et al., 2010b; Xiang and Wang, 2010; Zhang and Wang, 2015) and ribbon linking (Feinstein and Linstedt, 2008). GRASP55 and GRASP65 play complementary roles in Golgi structure formation, as single knockdown of GRASP55 or GRASP65 by siRNA, or knockout by CRISPR/Cas9, exhibit a mild effect on the Golgi structure, while double knockdown or knockout of both GRASP proteins causes the disassembly of both Golgi stack and ribbon structures (Bekier et al., 2017; Xiang and Wang, 2010; Xiang et al., 2013).

The Golgi structure is fragmented at the onset of mitosis and reassembled in telophase (Tang and Wang, 2013; Zhang and Wang, 2015). The process of Golgi cisternal unstacking at the onset of mitosis and restacking after its completion is known to be regulated by GRASP55 and GRASP65 phosphorylation (Duran et al., 2008; Feinstein and Linstedt, 2007; Xiang and Wang, 2010). In this study, we made an unexpected finding that SIRT2 interacts with and deacetylates GRASP55. Our results revealed a novel role for SIRT2 in Golgi structure formation through the modulation of GRASP55 acetylation levels, which affects GRASP55 self-interaction efficiency and post-mitotic Golgi reassembly.

## Results

### SIRT2 interacts with and deacetylates GRASP55

Our published SIRT2 interactome revealed that SIRT2 interacts with various Golgi proteins such as GRASP55 (also called GORASP2), Golgin-160 (GOLGA3) and GCP60 (ACBD3) (Kaufmann et al., 2016). GRASP55 ranked second in our interactome analysis and was identified by the proximity biotinylation (BioID) experiment in which SIRT2 was fused to a promiscuous biotin ligase from *E. coli* (BirA) at both the N- and the C-terminus (Roux et al., 2012). As BioID reveals mitotic interactors due to prolonged biotin-labeling (Lambert et al., 2015), we examined the interaction between SIRT2 and GRASP55 in asynchronous and nocodazole-arrested mitotic cells by co-immunoprecipitation. To preserve the acetylation state we included deacetylase inhibitors, trichostatin A and nicotinamide, in the lysis buffer. Our results showed that SIRT2 interacts with GRASP55 predominantly in mitosis (Figure 1A). Another Golgi protein, Golgin-84 (GOLGA5), did not show interaction with SIRT2 (Figure 1A), consistent with our mass spectrometry data that Golgin 84 ranked relatively low on the SIRT2 interactome list. Given that the endogenous SIRT2 protein level is very low (Supplemental Figure 1), we failed to detect the interaction between endogenous SIRT2 and GRASP55. Therefore, we performed reciprocal co-immunoprecipitation with HA-SIRT2, which exhibited strong interaction with

GRASP55 in mitosis (Figure 1B). These results confirm our mass spectrometry data and emphasize the value of BioID in revealing interactions that occur within specific stages of the cell cycle in an asynchronous cell population.

Since SIRT2 interacts with its substrate only when the substrate is acetylated, our results suggest that GRASP55 may be a SIRT2 target on the Golgi membranes. To determine whether SIRT2 directly deacetylates GRASP55, we performed *in vitro* acetylation and deacetylation assays using purified proteins. The acetylation level of GRASP55 was detected by an anti-acetyl lysine (AcK) antibody. GRASP55 was acetylated by p300 acetyltransferase and was deacetylated by wild-type (WT) SIRT2 (Figure 1C, lane 2 & 3) but not its catalytically inactive H150Y mutant (Figure 1C, lane 4 & 5) (Pandithage et al., 2008).

To determine the acetylation state of GRASP55 *in vivo,* we immunoprecipitated GRASP55-GFP from asynchronous or mitotic HEK293T cells and analyzed its acetylation by mass spectrometry. GRASP55 was found to be highly acetylated on K50 in mitosis (Supplemental Table 1). We then used parallel reaction monitoring (PRM) to analyze changes in GRASP55 acetylation at mitotic exit, as well as after SIRT2 depletion or overexpression in mitotic cells. GRASP55 K50 acetylation was significantly reduced at mitotic exit and after SIRT2 overexpression, whereas SIRT2 depletion further increased the K50 acetylation level in mitosis (Figure 1D; Supplemental Table 2). These results demonstrate that GRASP55 acetylation is regulated by SIRT2.

**SIRT2 depletion causes Golgi fragmentation**

The identification of GRASP55 as a novel SIRT2 substrate raised a possibility that SIRT2 may regulate Golgi morphology through GRASP55. To test the role of SIRT2 in Golgi structure formation, we depleted SIRT2 in HeLa and U2OS cells using siRNA and determined the effect on the Golgi morphology by immuno-staining GRASP55 and GM130. SIRT2 silencing caused Golgi fragmentation in both cell lines (Figure 2A-D), whereas overexpression of SIRT2 in WT cells had no significant effects on the Golgi morphology, although the Golgi appeared slightly more compact than that in control cells (Figure 2, E vs. B). In addition, the majority of cellular SIRT2 localized in the cytosol including the Golgi region (Figure 2E), consistent with its role in Golgi structure formation. To further understand the effect of SIRT2 depletion on the Golgi morphology, we analyzed the Golgi ultrastructure by electron microscopy (EM). The number of cisternae per Golgi stack and the length of cisternae were both significantly reduced in SIRT2-depleted cells (Figure 2F-H; Supplemental Figure 2), indicating that SIRT2 is required for proper maintenance of the Golgi structure.

Based on the fixed cell samples, we were unable to discern the cell cycle stage at which Golgi fragmentation occurred in SIRT2-depleted cells. Therefore, we generated a U2OS cell line stably expressing GRASP55-GFP and performed live-cell imaging to monitor the Golgi morphology in control and SIRT2-depleted cells during the cell cycle. Remarkably, SIRT2 silencing impaired post-mitotic Golgi reassembly (Figure 2I,J). While the Golgi was completely assembled 60 min after metaphase in WT cells, it remained as scattered fragments at 120 min in SIRT2-depleted cells (Figure 2I; Supplemental videos 1 and 2). Golgi fragmentation was 2-fold more pronounced in SIRT2-silenced cells than in control cells (Figure 2J), which correlates well with Golgi fragmentation analyzed by immunostaining of endogenous GRASP55 in SIRT2-depleted cells (Figure 2A-D).

**The deacetylase activity of SIRT2 is required for maintaining the Golgi structure**

To validate the specific effect of SIRT2 silencing on the Golgi morphology, we transfected SIRT2-depleted cells with RNAi resistant SIRT2 constructs. As shown in Figure 3A-C, expression of WT SIRT2, but not its inactive H150Y mutant, largely rescued Golgi fragmentation in SIRT2-depleted cells. These results indicate that the deacetylase activity of SIRT2 is required for maintaining the Golgi structure.

It has been previously shown that SIRT2 depletion may increase or decrease the protein levels of its substrates (Budayeva and Cristea, 2016). We therefore tested the effect of SIRT2 depletion or overexpression on the level of Golgi structural proteins by Western blot. Knockdown or overexpression of SIRT2 did not affect the level of various Golgi proteins tested in this experiment, including GRASP55, GRASP65, GM130, Golgin-160, and Golgin-84 (Figure 3D). This suggests that aberrant acetylation of Golgi proteins upon SIRT2 depletion causes Golgi fragmentation by perturbing protein-protein interactions rather than protein stability.

**GRASP55 deacetylation is required for post-mitotic Golgi structure formation**

Previous work showed that double knockdown or knockout of GRASP55 and GRASP65 causes the disassembly of both Golgi stack and ribbon structures (Bekier et al., 2017; Xiang and Wang, 2010; Xiang et al., 2013), whereas reintroduction of a single GRASP protein in GRASP55/65 double knockout cells can largely restore the Golgi structure (Bekier et al., 2017). To test whether aberrant acetylation of GRASP55 could be responsible for Golgi fragmentation in SIRT2-depleted cells, we generated K50R and K50Q mutants of GRASP55 to mimic hypo- and hyper-acetylation, respectively. Expression of these constructs did not affect GRASP55 phosphorylation in mitotic cells (Supplemental Figure 3). Consistent with previous reports, WT GRASP55-GFP, but not GFP alone, effectively

rescued the Golgi structure in GRASP55/65 double knockout HeLa cells (Figure 4). The acetylation-deficient K50R mutant restored the Golgi structure with similar efficiency as WT GRASP55, whereas the acetylation-mimetic K50Q mutant had a much weaker effect (Figure 4A-C).

Furthermore, we specifically examined the Golgi morphology in the later stages of mitosis in GRASP55/65 double knockout cells expressing GRASP55 WT, K50R and K50Q (Figure 5). In mitosis, the Golgi is disassembled into mitotic clusters (observed as dots under the microscope) and vesicles (observed as haze since the size of the vesicles is below the resolution of conventional microscopy). As cell cycle progresses, the Golgi structure reassembles in telophase and cytokinesis; the Golgi haze gradually disappears and the Golgi dots accumulate and merge into a single membrane complex. Expression of WT GRASP55, as well as the acetylation-deficient K50R mutant, accelerated Golgi reassembly in telophase and cytokinesis (Figure 5). Conversely, the acetylation-mimetic K50Q mutant was less effective in facilitating post-mitotic Golgi reassembly (Figure 5). This result is consistent with impaired post-mitotic Golgi reassembly caused by SIRT2 depletion, as shown in Figure 2I. Taken together, GRASP55 deacetylation is required for optimal Golgi structure formation, in particular at mitotic exit.

**The K50R acetylation-deficient mutant of GRASP55 partially rescues Golgi fragmentation caused by SIRT2 depletion**

Given that 1) GRASP55 is a substrate of the SIRT2 deacetylase (Figure 1), 2) SIRT2 depletion induces Golgi fragmentation (Figure 2,3), and 3) expression of the K50R acetylation-deficient GRASP55 mutant rescues Golgi fragmentation in GRASP55/65 double knockout cells (Figure 4,5), we further asked whether GRASP55 acetylation mutants could rescue the SIRT2 depletion phenotype. Therefore, we expressed GFP-tagged GRASP55 WT, K50R and K50Q in SIRT2-depleted cells. As shown in Figure 6, the acetylation-deficient K50R mutant exhibited a stronger effect than WT GRASP55 in rescuing the Golgi structure in SIRT2-depleted cells, whereas the acetylation-mimetic K50Q mutant had no effect. These results suggest that GRASP55 deacetylation by SIRT2 contributes to Golgi structure maintenance. The incomplete rescue of the Golgi structure by the acetylation-deficient K50R mutant indicates that SIRT2 may have additional substrates on the Golgi, or a cycle of acetylation and deacetylation may be required for Golgi structure formation.

**GRASP55 deacetylation facilitates self-interaction**

To address how GRASP55 acetylation may affect its function in Golgi structure formation, we probed the self-interaction efficiency of WT GRASP55 and its acetylation mutants (Figure 7). WT, K50R and K50Q GRASP55-GFP and GRASP55-FLAG were co-expressed, and synchronized mitotic cells were analyzed by GFP immunoprecipitation and anti-FLAG Western blotting. GRASP55 K50R showed higher self-interaction efficiency compared to WT or K50Q (Figure 7A-B, lane 7 vs. 6&8). Co-expression of GRASP55 K50R and K50Q exhibited an intermediate self-interaction efficiency, being lower compared to K50R-K50R but higher than K50Q-K50Q (Figure 7C-D, lanes 9&11 vs. 8 or 12). Reduced acetylation of GRASP55 therefore facilitates its self-interaction and contributes to post-mitotic Golgi structure formation.

**Discussion**

Recent proteomic analyses have revealed proteins in the endoplasmic reticulum and Golgi membrane networks as novel SIRT2 interacting partners (Budayeva and Cristea, 2016). In this study, we confirmed the interaction between SIRT2 and the Golgi reassembly stacking protein GRASP55, which occurs specifically in mitosis. We found that SIRT2 depletion not only increases GRASP55 acetylation level but also induces Golgi fragmentation and impairs post-mitotic Golgi reassembly. Furthermore, we discovered that GRASP55 is highly acetylated in mitosis on K50 and deacetylated at mitotic exit, indicating that SIRT2 regulates Golgi structure formation by deacetylating GRASP55 at the end of mitosis. Importantly, expression of WT or the acetylation-deficient K50R mutant of GRASP55, but not the acetylation-mimetic K50Q mutant, rescued Golgi fragmentation and restored post-mitotic Golgi reassembly in GRASP55/65 double knockout cells, indicating that GRASP55 deacetylation is required for post-mitotic Golgi structure formation. Acetylation of GRASP55 in mitosis presumably facilitates Golgi disassembly, whereas its deacetylation is clearly required for proper Golgi reassembly at the mitotic exit. Indeed, acetylation-deficient GRASP55 has higher self-interaction efficiency, which facilitates Golgi reassembly. Thus, our study revealed acetylation as a novel mechanism that regulates Golgi structure formation.

There is a growing number of proteins similar to GRASP55 that undergo cell cycle-dependent changes in acetylation. For example, histone H4 is highly acetylated at K16 during S phase and deacetylated by SIRT2 at the G2/M transition (Vaquero et al., 2006); cyclin A acetylation in mitosis targets it for ubiquitination and subsequent degradation (Mateo et al., 2009); ANKLE2 is highly acetylated in mitosis and the regulation of its acetylation state by SIRT2 is necessary for proper nuclear envelope reassembly at the end of mitosis (Kaufmann et al., 2016). Acetylation is highly abundant

during mitosis (Chuang et al., 2010) and will doubtlessly continue to emerge as a post-translational protein modification that regulates cell cycle progression. Cell-cycle regulation of protein acetylation necessitates tight regulation of deacetylases; phosphorylation during mitosis stabilizes SIRT2, whereas dephosphorylation at the mitotic exit leads to proteasome-mediated degradation (Dryden et al., 2003; North and Verdin, 2007).

It has been reported that tubulin acetylation on kinetochore microtubules in the mitotic spindle is regulated by SIRT2 (Nagai et al., 2013). Given that microtubule cytoskeleton is required for an intact Golgi, this raises a concern that SIRT2 may regulate the Golgi structure through microtubules. However, expression of the GRASP55 K50R mutant largely rescues the Golgi structure in SIRT2-depleted cells, suggesting that SIRT2 directly regulates Golgi structure through GRASP55.

Identifying SIRT2 deacetylase substrates within the ER-Golgi network raises a question where and how these substrates are initially acetylated. Lysine acetylation can occur in the lumen of the ER (Pehar and Puglielli, 2013), while the Golgi lumen is known to possess deacetylase activity (Costantini et al., 2007). Transient acetylation of ER membrane proteins seems to facilitate protein folding by neutralizing the positive charge in kinetically unfavorable areas of the nascent protein and may protect correctly folded proteins from disposal (Pehar and Puglielli, 2013). For example, transient acetylation of the nascent ER form of the β-secretase BACE1 is required for its maturation within the Golgi apparatus where it is deacetylated (Costantini et al., 2007). However, unlike secretory and membrane proteins that are synthesized by the ER and transported to the Golgi, GRASP55 is a peripheral membrane protein on the cytoplasmic surface of the Golgi. While we showed that p300 acetyltransferase can acetylate GRASP55 *in vitro*, the acetylation mechanism *in vivo* will be a subject for future investigation.

Golgi fragmentation accelerates protein trafficking by enhancing vesicle budding from the Golgi membranes in interphase cells (Wang et al., 2008; Zhang and Wang, 2015). Fragmentation of the Golgi apparatus is associated with neurodegenerative diseases such as Alzheimer's and Parkinson's (Fujita et al., 2006; Gonatas et al., 2006; Joshi and Wang, 2015). In Alzheimer's disease, Golgi fragmentation was linked to GRASP65 phosphorylation by the Cdk5 kinase, which results in increased trafficking of the amyloid precursor protein (APP) and increased amyloid beta (Aβ) production (Joshi et al., 2014; Joshi and Wang, 2015). In Parkinson's disease, Golgi fragmentation was linked with altered levels of Rab proteins and the SNARE protein syntaxin 5, and precedes α-synuclein aggregation (Rendon et al., 2013). Interestingly, SIRT2 is also implicated in neurodegenerative diseases and SIRT2 inhibition was shown to have a neuroprotective effect in various Parkinson's disease models (Chen et al., 2015; Godena et al., 2014; Outeiro et al., 2007) and in Alzheimer's disease (Silva et al., 2016). It would thus be interesting

to examine Golgi morphology in neurodegenerative disease models following SIRT2 depletion or inhibition.

While our results indicate that GRASP55 is a specific target of SIRT2 through which SIRT2 regulates Golgi morphology, future work may still be needed to characterize other potential SIRT2 targets within the Golgi network.

## Materials and Methods

### Cell lines

Tissue culture media, supplements, and antibiotics were purchased from Sigma or Invitrogen. Bovine serum was obtained from Sigma or Gemini. All cell lines were maintained in Dulbecco's Modified Eagle's Medium (DMEM 4.5 g/L glucose) supplemented with 10% fetal bovine serum, 1% L-glutamine, 1% penicillin-streptomycin under 5% $CO_2$ at 37°C. HEK293T (ATCC, CRL-3216) and HeLa cells (ATCC, CCL-2) were used for transient transfections. To obtain mitotic cells, HEK293T and HeLa cells were treated with 330 nM nocodazole (Sigma) for 18 h. U2OS cells (gift from Dr. Xiaochun Yu, City of Hope National Medical Center) stably expressing GRASP55-GFP were generated by transfection of the respective plasmid and selection of stable clones in the presence of 400 µg/ml G418 (Sigma). Transfection was performed with polyethylenimine (PEI; Polysciences).

### Plasmids and proteins

The cloning and expression of SIRT2 and p300 acetyltransferase were described previously (Kaufmann et al., 2016). Human GRASP55 was cloned into pDEST N3xFLAG from pDONR23 (human ORFeome 5.1 collection; kindly provided by Ivana Grbesa). Rat GRASP55 was cloned into pEGFP-N1 between BglII and HindIII for mammalian expression and into pET23 (Novagen) for bacterial expression (Zhang et al., 2019; Zhang et al., 2018). RNAi resistant SIRT2 constructs were generated by site-directed mutagenesis according to the FastCloning protocol (Li et al., 2011) using the following primers: 5'- ACCAAAATGCGAGGATTGTCAGAGCCTGGTGAAGCCTGATATCGTC-3' and 5'-CAATCCTCGCATTTTGGTGTCACCTCAGAGAAGATCTTCTCTTTCA-3'. All new cDNA constructs were confirmed by DNA sequencing. Proteins were expressed in *E. coli* Rosetta2 (DE3) cells (Novagen). His-tagged GRASP55 was purified on HisPur Ni-NTA Resin (Pierce, Thermo Scientific) according to a standard procedure (Zhang et al., 2018).

## Antibodies

The following antibodies were used for Western blotting: rabbit anti-SIRT2 (1:1000; Cell Signaling, 12650), rabbit anti-GRASP55 (1:2000; Proteintech, 10598-1-AP), mouse anti-GM130 (1:2000; BD Transduction Laboratories, 610823), rabbit anti-GRASP65 (1:2000; a kind gift from Joachim Seeman), rabbit anti-Golgin 160 (1:2000; Proteintech, 21193-1-AP), rabbit anti-Golgin 84 (1:3000; a kind gift from Ayano Satoh), anti-FLAG M2-peroxidase clone M2 (1:10000; Sigma, A8592), mouse anti-HA.11 clone 16B12 (1:1000; Covance, MMS-101R), mouse anti-myc clone 4A6 (1:1000; Merck Millipore, 05-724), rabbit anti-acetylated-lysine (AcK, 1:1000; Cell Signaling, 9441), mouse anti-His (1:5000; GE Healthcare, 27-4710-01), mouse anti-GFP (1:1000; Roche, 11814460001), rabbit anti-actin (1:10000; Sigma, A2066). The following antibodies were used for immunofluorescence: rabbit anti-GRASP55 (1:200; Proteintech, 10598-1-AP), mouse anti-GM130 (1:200; BD Transduction Laboratories, 610823). Secondary HRP-conjugated antibodies for Western blotting (Jackson ImmunoResearch) were used at 1:10000 dilution. Secondary FITC- or TRITC-conjugated antibodies for immunofluorescence (Jackson ImmunoResearch) were used at 1:100 dilution.

## RNA interference

SiRNA transfections were performed using Lipofectamine RNAiMax (Ambion, Life Technologies) according to the manufacturer's instructions. SIRT2 siRNAs used for immunofluorescence analysis and live cell imaging were from Invitrogen (Silencer® Select; 5'-GCCCAAGTGTGAAGACTGT-3') and Dharmacon (SMARTpool ON-TARGETplus), respectively. Cells were transfected with siRNAs at a final concentration of 50 nM and assayed 72 h after transfection.

## Mass spectrometry analysis of GRASP55 acetylation

GRASP55-GFP was transfected into HEK293T cells and immunoprecipitated using GFP-Trap magnetic beads (Chromotek). Bands were excised from silver-stained gels and submitted to mass spectrometry analysis as described in (Kaufmann et al., 2017) except that 20 mM iodoacetamide was used as alkylating reagent before digesting the proteins with trypsin (Trypsin Gold, Promega). Samples analyzed by parallel reaction monitoring (PRM) were spiked with 100 fmol Pierce Retention Time Calibration standard (PRTC, Thermo Fisher Scientific) per injection for quality control and retention time monitoring. PRM assay generation was performed using Skyline (MacLean et al., 2010), resulting in a scheduled assay with 12 min windows and not more than eight concurrent precursors per window.

For data acquisition we operated an Ultimate 3000 RSLC nano-flow chromatography system (Thermo Fisher Scientific), using a pre-column for sample loading (PepMapAcclaim C18, 2 cm × 0.1 mm, 5 µm, Thermo Fisher Scientific), and a C18 analytical column (PepMapAcclaim C18, 50 cm × 0.75 mm, 2 µm, Thermo Fisher Scientific), applying a linear gradient from 2% to 30% solvent B (80% acetonitrile, 0.1% formic acid; solvent A 0.1% formic acid) at a flow rate of 230 nl/min over 60 min. Eluted peptides were analyzed on a Q Exactive HF Orbitrap mass spectrometer (Thermo Fisher Scientific), equipped with a Proxeon nano-spray-source (Thermo Fisher Scientific). MS parameters: survey scan with 60k resolution, AGC 1E6, 50 ms IT, over a range of 380 to 1100 m/z; PRM scan with 60k resolution, AGC 2E5, 250 ms IT, isolation window of 0.7 m/z with 0.2 m/z offset, and NCE of 27%.

The spectral library for PRM data analysis in Skyline was generated as follows: a spectral library was prepared in Proteome Discoverer (Thermo Fisher Scientific, version 2.3) using MS Amanda (Dorfer et al., 2014) and Percolator (Kall et al., 2007) with the following search parameters: database compiled of the *Rattus norvegicus* reference Proteome (UniProt, April 2019) and common contaminants, 10 ppm MS1 and 20 ppm MS2 mass tolerance, carbamidomethylation of Cys as fixed and Lys acetylation and Met oxidation as variable modifications, three missed cleavages allowed, 1% FDR on PSM level. Results were imported into Skyline using a score cut-off of 0.95 and filtering for GRASP55 peptides.

Data analysis, including manual validation of all peptides and their transitions (based on MS2 spectra, retention time, relative ion intensities, and mass accuracy), and relative quantification was performed in Skyline. Six of the most intense non-interfering transitions of the target peptides were selected and their peak areas were summed for peptide quantification (total peak area). As a quality control for instrument performance, PRTC peptides were monitored using MS1-full scan filtering. Peak areas were exported from Skyline. To allow a relative quantitative comparison of K50ac independent of GRASP55 abundance we normalized the intensity of the peptide LNKacDNDTLK to the intensity of its non-modified counter-peptide LNKDNDTLK. Although such an approach is usually problematic due to the missed tryptic cleavage on acetyl-Lys residues, it is reasonable in this case because the Asp residue in the +1 position suppresses cleavage to an extent large enough to provide a peptide signal one order of magnitude higher than in its acetylated form.

### *In vitro* acetylation and deacetylation assays

*In vitro* acetylation assay was performed by incubating 5 µg human $His_6$-tagged GRASP55 with 0.5 µg of p300 acetyltransferase (Kaufmann et al., 2016) in 50 µl of 10 µM acetyl-CoA (Sigma), 50 mM Tris-Cl pH8.0, 10% glycerol, 0.1 mM EDTA, 1 mM DTT and 1 mM PMSF for 2 h at 30°C with rotation. The acetylation reaction was stopped with 20 µM anacardic acid. Subsequent *in vitro* deacetylation assay was performed by adding 0.5 or 5 µg His-tagged SIRT2 WT or its catalytically inactive H150Y mutant (Kaufmann et al., 2016) and incubating for 90 min at 37°C. The acetylation levels of GRASP55 and p300 was detected by an anti-acetyl lysine antibody (AcK, Cell Signaling).

### Immunoprecipitation

To determine the interaction between FLAG-SIRT2 and GRASP55-GFP, transfected HeLa cells were lysed at 4°C for 20 min in 20 mM Tris-Cl pH8.0, 150 mM NaCl, 1% Triton X-100, 20 mM beta-phosphoglycerol, 10 µM trichostatin A (TSA; Sigma), 20 mM nicotinamide (NAM; Sigma) and protease inhibitors. Cell lysates were rotated with anti-GFP antibodies coupled to magnetic beads (GFP-Trap_M, Chromotek) for 2 h at 4°C. Beads were washed five times with the lysis buffer and eluted by boiling, samples were then subjected to Western blotting.

To determine the interaction between HA-SIRT2 and FLAG-GRASP55, cells were harvested by scraping and cell pellets were lysed in the lysis buffer containing 50 mM Tris-HCl pH8.0, 150 mM NaCl, 1% Triton X-100, 50 U/ml benzonase (Novagen), protease inhibitors (Complete Mini Protease Inhibitor Cocktail Tablets, EDTA-free; Roche), 5 µM TSA (Sigma), 20 mM NAM (Sigma) for 1 h with rotation at 4°C. Anti-HA magnetic beads (Pierce) were equilibrated by washing the beads twice with TBS (Tris-buffered saline). Lysates were incubated with the beads for 2 h at 4°C with rotation. Beads were washed three times with the lysis buffer and eluted with glycine pH2.0, samples were then subjected to Western blotting.

To determine the self-interaction efficiency of GRASP55 WT or its acetylation mutants K50R and K50Q, HeLa cells were transfected with indicated plasmids, synchronized with nocodazole for 18 h, and lysed in 20 mM Tris-HCl, pH 8.0, 150 mM NaCl, 1% Triton X-100 and protease inhibitors. Lysates were cleared by centrifugation, incubated with GFP antibodies overnight at 4°C, subsequently incubated with protein A beads for another 2 h, reisolated and analyzed by Western blotting.

**Immunofluorescence**

Cells were grown on sterile glass coverslips, rinsed with PBS, fixed in 4% paraformaldehyde for 10 min and permeabilized with 0.3% Triton X-100 in PBS for 5 min. Cells were subsequently blocked in 0.2% gelatin in PBS for 15 min, incubated with primary antibodies for 45 min, washed and probed with the appropriate secondary antibodies conjugated to FITC or TRITC for 45 min. DNA was stained with Hoechst for 5 min, rinsed with PBS, mounted with Mowiol onto slides and sealed with nail polish. Images of the samples were taken with a 63x oil objective on a Zeiss Observer Z1 epifluorescence microscope. Axiovert software was used for image acquisition and analysis.

**Live cell imaging**

Cells were seeded in multi-well dishes or 6-channel slides suitable for high resolution microscopy (Ibidi) the day before imaging. Live cell imaging was performed on an Axio Observer Z1 (Zeiss) equipped with an EM-CCD camera (Evolve EM-512) and environmental control.

**Electron microscopy (EM)**

EM was performed as previously described (Tang et al., 2010a). Briefly, HeLa cells were transfected with control and SIRT2 RNAi for 72 h, and then plated in six-well dishes. After another 24 h culture, cells were processed for Epon embedding. Sections of 60 nm were mounted onto Formvar-coated nickel grids and stained with 2% uranyl acetate for 5 min and 3% lead citrate for another 5 min. Grids were imaged using a JOEL transmission electron microscope. Images from >25 cells were captured at 10,000x magnification and were taken from the perinuclear region of the cell where Golgi membranes were normally concentrated. A cisterna was defined as a membrane-bound structure in the Golgi cluster whose length is at least 4 times its width, and the latter does not exceed 60 nm; a stack is the set of flattened, disk-shaped cisternae piling up together. The longest cisternae in a Golgi stack were measured as the length of cisternae using ImageJ, and the number of cisternae in the Golgi stack with the most cisternae layers was counted as the number of cisternae per stack (Wang et al., 2005). In our assays, defects in Golgi stack formation are reflected as 1) a reduced number of cisternae per stack, and 2) improper alignment of the cisternae within each stack accompanied with increased number of vesicles.

### Quantification and statistics

Error bars represent standard error of mean (SEM) estimated from two to four independent experiments. Statistical significance was calculated using a two-tailed t-test. P-values smaller than 0.05 were considered statistically significant and indicated with an asterisk (*, for $p<0.05$; **, for $p<0.01$; ***, for $p<0.001$). Fragmented Golgi was defined as disconnected or scattered dots. To quantify the percentage of fixed cells with fragmented Golgi, we counted more than 200 cells in each treatment. To quantify the percentage of live cells with fragmented Golgi, we counted more than 40 cells in each treatment. To determine the Golgi phenotype with EM, we counted the number of cisternae per stack or the length of Golgi cisternae from 20 different control RNAi cells or SIRT2 RNAi cells.


### Acknowledgments

We thank Dr. Markus Hartl, Natascha Hartl, Karl Mechtler and Etienne Beltzung for mass spectrometry analysis of GRASP55 PTMs. We thank Dr. Ivana Grbesa for the human GRASP55 construct, Drs. Ayano Satoh, Joachim Seeman and Xiaochun Yu for antibodies and U2OS cells, and other members of the Slade and Wang labs for suggestions, reagents and technical support.

### Competing interests

The authors declare no competing or financial interests.

### Funding

This work was supported in part by the National Institutes of Health (Grants GM112786, GM105920 and GM130331), MCubed and the Fast Forward Protein Folding Disease Initiative of the University of Michigan to YW, and by the MFPL start-up and the WWTF LS14-001 grant to DS.


### Authorship

XZ performed and analyzed experiments in Figure 1A, 2A-H, 3-7, as well as Supplemental Figure 1-3, and wrote the manuscript; AB performed and analyzed experiments in Figure 2I-J; DS and EK performed MS analysis of GRASP55 acetylation; DS conceived the study, performed experiments in Figure 1B-D, analyzed data and wrote the manuscript; YW conceived the study, analyzed data and wrote the manuscript.

## References


**Bekier, M. E., 2nd, Wang, L., Li, J., Huang, H., Tang, D., Zhang, X. and Wang, Y.** (2017). Knockout of the Golgi stacking proteins GRASP55 and GRASP65 impairs Golgi structure and function. *Mol Biol Cell* **28**, 2833-2842.

**Bosch-Presegue, L. and Vaquero, A.** (2011). The dual role of sirtuins in cancer. *Genes Cancer* **2**, 648-62.

**Budayeva, H. G. and Cristea, I. M.** (2016). Human Sirtuin 2 Localization, Transient Interactions, and Impact on the Proteome Point to Its Role in Intracellular Trafficking. *Mol Cell Proteomics* **15**, 3107-3125.

**Chen, X., Wales, P., Quinti, L., Zuo, F., Moniot, S., Herisson, F., Rauf, N. A., Wang, H., Silverman, R. B., Ayata, C. et al.** (2015). The sirtuin-2 inhibitor AK7 is neuroprotective in models of Parkinson's disease but not amyotrophic lateral sclerosis and cerebral ischemia. *PLoS One* **10**, e0116919.

**Chuang, C., Lin, S. H., Huang, F., Pan, J., Josic, D. and Yu-Lee, L. Y.** (2010). Acetylation of RNA processing proteins and cell cycle proteins in mitosis. *J Proteome Res* **9**, 4554-64.

**Costantini, C., Ko, M. H., Jonas, M. C. and Puglielli, L.** (2007). A reversible form of lysine acetylation in the ER and Golgi lumen controls the molecular stabilization of BACE1. *Biochem J* **407**, 383-95.

**Dorfer, V., Pichler, P., Stranzl, T., Stadlmann, J., Taus, T., Winkler, S. and Mechtler, K.** (2014). MS Amanda, a universal identification algorithm optimized for high accuracy tandem mass spectra. *J Proteome Res* **13**, 3679-84.

**Dryden, S. C., Nahhas, F. A., Nowak, J. E., Goustin, A. S. and Tainsky, M. A.** (2003). Role for human SIRT2 NAD-dependent deacetylase activity in control of mitotic exit in the cell cycle. *Mol Cell Biol* **23**, 3173-85.

**Duran, J. M., Kinseth, M., Bossard, C., Rose, D. W., Polishchuk, R., Wu, C. C., Yates, J., Zimmerman, T. and Malhotra, V.** (2008). The Role of GRASP55 in Golgi Fragmentation and Entry of Cells into Mitosis. *Mol Biol Cell* **19**, 2579-87.

**Feinstein, T. N. and Linstedt, A. D.** (2007). Mitogen-activated protein kinase kinase 1-dependent Golgi unlinking occurs in G2 phase and promotes the G2/M cell cycle transition. *Mol Biol Cell* **18**, 594-604.

**Feinstein, T. N. and Linstedt, A. D.** (2008). GRASP55 Regulates Golgi Ribbon Formation. *Mol Biol Cell* **19**, 2696-707.

**Fujita, Y., Ohama, E., Takatama, M., Al-Sarraj, S. and Okamoto, K.** (2006). Fragmentation of Golgi apparatus of nigral neurons with alpha-synuclein-positive inclusions in patients with Parkinson's disease. *Acta Neuropathol* **112**, 261-5.

**Godena, V. K., Brookes-Hocking, N., Moller, A., Shaw, G., Oswald, M., Sancho, R. M., Miller, C. C., Whitworth, A. J. and De Vos, K. J.** (2014). Increasing microtubule acetylation rescues axonal transport and locomotor deficits caused by LRRK2 Roc-COR domain mutations. *Nat Commun* **5**, 5245.

**Gonatas, N. K., Stieber, A. and Gonatas, J. O.** (2006). Fragmentation of the Golgi apparatus in neurodegenerative diseases and cell death. *J Neurol Sci* **246**, 21-30.

**Harting, K. and Knoll, B.** (2010). SIRT2-mediated protein deacetylation: An emerging key regulator in brain physiology and pathology. *Eur J Cell Biol* **89**, 262-9.

**Inoue, T., Hiratsuka, M., Osaki, M., Yamada, H., Kishimoto, I., Yamaguchi, S., Nakano, S., Katoh, M., Ito, H. and Oshimura, M.** (2007). SIRT2, a tubulin deacetylase, acts to block the entry to chromosome condensation in response to mitotic stress. *Oncogene* **26**, 945-57.

**Janke, C.** (2014). The tubulin code: molecular components, readout mechanisms, and functions. *J Cell Biol* **206**, 461-72.

**Jin, Y. H., Kim, Y. J., Kim, D. W., Baek, K. H., Kang, B. Y., Yeo, C. Y. and Lee, K. Y.** (2008). Sirt2 interacts with 14-3-3 beta/gamma and down-regulates the activity of p53. *Biochem Biophys Res Commun* **368**, 690-5.

**Jing, E., Gesta, S. and Kahn, C. R.** (2007). SIRT2 regulates adipocyte differentiation through FoxO1 acetylation/deacetylation. *Cell Metab* **6**, 105-14.

**Joshi, G., Chi, Y., Huang, Z. and Wang, Y.** (2014). Abeta-induced Golgi fragmentation in Alzheimer's disease enhances Abeta production. *Proc Natl Acad Sci U S A* **111**, E1230-9.

**Joshi, G. and Wang, Y.** (2015). Golgi defects enhance APP amyloidogenic processing in Alzheimer's disease. *Bioessays* **37**, 240-7.

**Kall, L., Canterbury, J. D., Weston, J., Noble, W. S. and MacCoss, M. J.** (2007). Semi-supervised learning for peptide identification from shotgun proteomics datasets. *Nat Methods* **4**, 923-5.

**Kaufmann, T., Grishkovskaya, I., Polyansky, A. A., Kostrhon, S., Kukolj, E., Olek, K. M., Herbert, S., Beltzung, E., Mechtler, K., Peterbauer, T. et al.** (2017). A novel non-canonical PIP-box mediates PARG interaction with PCNA. *Nucleic Acids Res* **45**, 9741-9759.

**Kaufmann, T., Kukolj, E., Brachner, A., Beltzung, E., Bruno, M., Kostrhon, S., Opravil, S., Hudecz, O., Mechtler, K., Warren, G. et al.** (2016). SIRT2 regulates nuclear envelope reassembly through ANKLE2 deacetylation. *J Cell Sci* **129**, 4607-4621.

**Kim, H. S., Vassilopoulos, A., Wang, R. H., Lahusen, T., Xiao, Z., Xu, X., Li, C., Veenstra, T. D., Li, B., Yu, H. et al.** (2011). SIRT2 maintains genome integrity and suppresses tumorigenesis through regulating APC/C activity. *Cancer Cell* **20**, 487-99.

**Lambert, J. P., Tucholska, M., Go, C., Knight, J. D. and Gingras, A. C.** (2015). Proximity biotinylation and affinity purification are complementary approaches for the interactome mapping of chromatin-associated protein complexes. *J Proteomics* **118**, 81-94.

**Li, C., Wen, A., Shen, B., Lu, J., Huang, Y. and Chang, Y.** (2011). FastCloning: a highly simplified, purification-free, sequence- and ligation-independent PCR cloning method. *BMC Biotechnol* **11**, 92.

**Lin, R., Tao, R., Gao, X., Li, T., Zhou, X., Guan, K. L., Xiong, Y. and Lei, Q. Y.** (2013). Acetylation stabilizes ATP-citrate lyase to promote lipid biosynthesis and tumor growth. *Mol Cell* **51**, 506-18.

**MacLean, B., Tomazela, D. M., Shulman, N., Chambers, M., Finney, G. L., Frewen, B., Kern, R., Tabb, D. L., Liebler, D. C. and MacCoss, M. J.** (2010). Skyline: an open source document editor for creating and analyzing targeted proteomics experiments. *Bioinformatics* **26**, 966-8.

**Mateo, F., Vidal-Laliena, M., Canela, N., Busino, L., Martinez-Balbas, M. A., Pagano, M., Agell, N. and Bachs, O.** (2009). Degradation of cyclin A is regulated by acetylation. *Oncogene* **28**, 2654-66.

**Nagai, T., Ikeda, M., Chiba, S., Kanno, S. and Mizuno, K.** (2013). Furry promotes acetylation of microtubules in the mitotic spindle by inhibition of SIRT2 tubulin deacetylase. *J Cell Sci* **126**, 4369-80.

**North, B. J., Marshall, B. L., Borra, M. T., Denu, J. M. and Verdin, E.** (2003). The human Sir2 ortholog, SIRT2, is an NAD+-dependent tubulin deacetylase. *Mol Cell* **11**, 437-44.

**North, B. J. and Verdin, E.** (2007). Interphase nucleo-cytoplasmic shuttling and localization of SIRT2 during mitosis. *PLoS One* **2**, e784.

**Outeiro, T. F., Kontopoulos, E., Altmann, S. M., Kufareva, I., Strathearn, K. E., Amore, A. M., Volk, C. B., Maxwell, M. M., Rochet, J. C., McLean, P. J. et al.** (2007). Sirtuin 2 inhibitors rescue alpha-synuclein-mediated toxicity in models of Parkinson's disease. *Science* **317**, 516-9.

**Pandithage, R., Lilischkis, R., Harting, K., Wolf, A., Jedamzik, B., Luscher-Firzlaff, J., Vervoorts, J., Lasonder, E., Kremmer, E., Knoll, B. et al.** (2008). The regulation of SIRT2 function by cyclin-dependent kinases affects cell motility. *J Cell Biol* **180**, 915-29.

**Pehar, M. and Puglielli, L.** (2013). Lysine acetylation in the lumen of the ER: a novel and essential function under the control of the UPR. *Biochim Biophys Acta* **1833**, 686-97.

**Rendon, W. O., Martinez-Alonso, E., Tomas, M., Martinez-Martinez, N. and Martinez-Menarguez, J. A.** (2013). Golgi fragmentation is Rab and SNARE dependent in cellular models of Parkinson's disease. *Histochem Cell Biol* **139**, 671-84.

**Rothgiesser, K. M., Erener, S., Waibel, S., Luscher, B. and Hottiger, M. O.** (2010). SIRT2 regulates NF-kappaB dependent gene expression through deacetylation of p65 Lys310. *J Cell Sci* **123**, 4251-8.

**Roux, K. J., Kim, D. I., Raida, M. and Burke, B.** (2012). A promiscuous biotin ligase fusion protein identifies proximal and interacting proteins in mammalian cells. *J Cell Biol* **196**, 801-10.

**Serrano, L., Martinez-Redondo, P., Marazuela-Duque, A., Vazquez, B. N., Dooley, S. J., Voigt, P., Beck, D. B., Kane-Goldsmith, N., Tong, Q., Rabanal, R. M. et al.** (2013). The tumor suppressor SirT2 regulates cell cycle progression and genome stability by modulating the mitotic deposition of H4K20 methylation. *Genes Dev* **27**, 639-53.

**Shorter, J., Watson, R., Giannakou, M. E., Clarke, M., Warren, G. and Barr, F. A.** (1999). GRASP55, a second mammalian GRASP protein involved in the stacking of Golgi cisternae in a cell-free system. *EMBO J* **18**, 4949-4960.

**Silva, D. F., Esteves, A. R., Oliveira, C. R. and Cardoso, S. M.** (2016). Mitochondrial Metabolism Power SIRT2-Dependent Deficient Traffic Causing Alzheimer's-Disease Related Pathology. *Mol Neurobiol*.

**Tang, D. and Wang, Y.** (2013). Cell cycle regulation of Golgi membrane dynamics. *Trends Cell Biol* **23**, 296-304.

**Tang, D., Xiang, Y. and Wang, Y.** (2010a). Reconstitution of the cell cycle-regulated Golgi disassembly and reassembly in a cell-free system. *Nature protocols* **5**, 758-72.

**Tang, D., Yuan, H. and Wang, Y.** (2010b). The Role of GRASP65 in Golgi Cisternal Stacking and Cell Cycle Progression. *Traffic* **11**, 827-42.

**Tsusaka, T., Guo, T., Yagura, T., Inoue, T., Yokode, M., Inagaki, N. and Kondoh, H.** (2014). Deacetylation of phosphoglycerate mutase in its distinct central region by SIRT2 down-regulates its enzymatic activity. *Genes Cells* **19**, 766-77.

**Vaquero, A., Scher, M. B., Lee, D. H., Sutton, A., Cheng, H. L., Alt, F. W., Serrano, L., Sternglanz, R. and Reinberg, D.** (2006). SirT2 is a histone deacetylase with preference for histone H4 Lys 16 during mitosis. *Genes Dev* **20**, 1256-61.

**Wang, Y., Satoh, A. and Warren, G.** (2005). Mapping the functional domains of the Golgi stacking factor GRASP65. *J Biol Chem* **280**, 4921-8.

**Wang, Y., Seemann, J., Pypaert, M., Shorter, J. and Warren, G.** (2003). A direct role for GRASP65 as a mitotically regulated Golgi stacking factor. *EMBO J* **22**, 3279-90.

**Wang, Y., Wei, J. H., Bisel, B., Tang, D. and Seemann, J.** (2008). Golgi Cisternal Unstacking Stimulates COPI Vesicle Budding and Protein Transport. *PLoS One* **3**, e1647.

**Xiang, Y. and Wang, Y.** (2010). GRASP55 and GRASP65 play complementary and essential roles in Golgi cisternal stacking. *J Cell Biol* **188**, 237-51.

**Xiang, Y., Zhang, X., Nix, D. B., Katoh, T., Aoki, K., Tiemeyer, M. and Wang, Y.** (2013). Regulation of protein glycosylation and sorting by the Golgi matrix proteins GRASP55/65. *Nat Commun* **4**, 1659.

**Zhang, H., Head, P. E., Daddacha, W., Park, S. H., Li, X., Pan, Y., Madden, M. Z., Duong, D. M., Xie, M., Yu, B. et al.** (2016). ATRIP Deacetylation by SIRT2 Drives ATR Checkpoint Activation by Promoting Binding to RPA-ssDNA. *Cell Rep* **14**, 1435-47.

**Zhang, H., Park, S. H., Pantazides, B. G., Karpiuk, O., Warren, M. D., Hardy, C. W., Duong, D. M., Park, S. J., Kim, H. S., Vassilopoulos, A. et al.** (2013). SIRT2 directs the replication stress response through CDK9 deacetylation. *Proc Natl Acad Sci U S A* **110**, 13546-51.

**Zhang, X., Wang, L., Ireland, S. C., Ahat, E., Li, J., Bekier Ii, M. E., Zhang, Z. and Wang, Y.** (2019). GORASP2/GRASP55 collaborates with the PtdIns3K UVRAG complex to facilitate autophagosome-lysosome fusion. *Autophagy*, 1-14.

**Zhang, X., Wang, L., Lak, B., Li, J., Jokitalo, E. and Wang, Y.** (2018). GRASP55 Senses Glucose Deprivation through O-GlcNAcylation to Promote Autophagosome-Lysosome Fusion. *Dev Cell* **45**, 245-261 e6.

**Zhang, X. and Wang, Y.** (2015). GRASPs in Golgi Structure and Function. *Frontiers in Cell and Developmental Biology* **3**, 84.

**Zhang, X. and Wang, Y.** (2016). Glycosylation Quality Control by the Golgi Structure. *J Mol Biol* **428**, 3183-93.

**Figures**

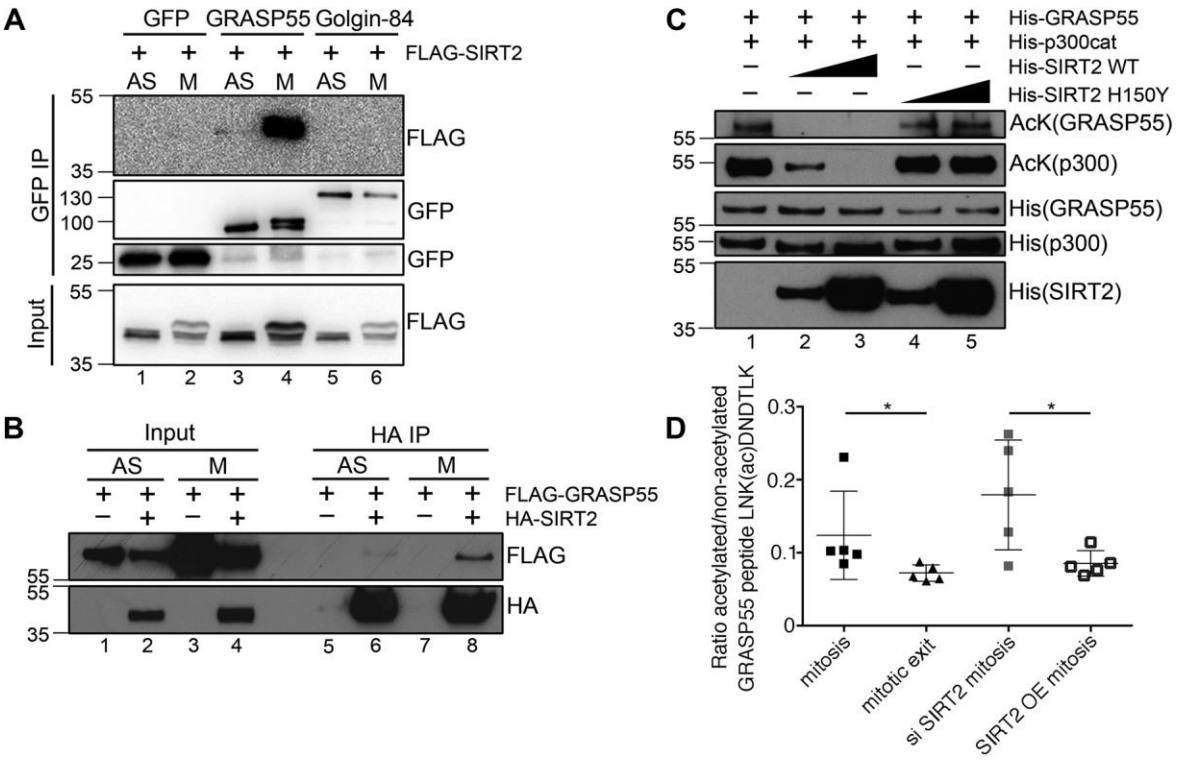


**Figure 1. SIRT2 interacts with GRASP55 in mitosis and deacetylates GRASP55 at mitotic exit.** **A.** SIRT2 co-immunoprecipitates with GRASP55 but not Golgin-84 in mitosis. Asynchronous (AS) and nocodazole-arrested mitotic HeLa cells co-overexpressing GFP-tagged GRASP55 or Golgin-84 and FLAG-SIRT2 were lysed, immunoprecipitated with a GFP antibody, and blotted for GFP and FLAG. The upper bands of FLAG-SIRT2 and GRASP55-GFP in mitotic samples correspond to their phosphorylated forms. **B.** Western blots of HA immunoprecipitation from HEK293T cells expressing HA-SIRT2 and FLAG-GRASP55. **C.** *In vitro* acetylation of GRASP55 with p300 acetyltransferase and deacetylation of GRASP55 by SIRT2. 1.5 µg of GRASP55, 0.15 µg of p300 acetyltransferase and 0.15/1.5 µg of SIRT2 or SIRT2 H150Y were present in the loaded samples. Acetylation level of GRASP55 and p300 was detected by an anti-acetyl lysine (AcK) antibody. **D.** Targeted mass spectrometry analysis of GRASP55 K50 acetylation in HEK293T cells transfected with GRASP55-GFP. Mitotic samples were collected after 16 h synchronization with nocodazole. Mitotic exit samples were collected 2 h after release from nocodazole. SIRT2 siRNA was transfected for 72 h. HA-SIRT2 was overexpressed for 24 h. K50 acetylation level was determined as a ratio between modified and unmodified LNK(ac)DNDTLK peptide (n=5). Quantification results are presented as mean ± SEM. Statistics was performed using two-tailed Student's t-test. *, $p < 0.05$.

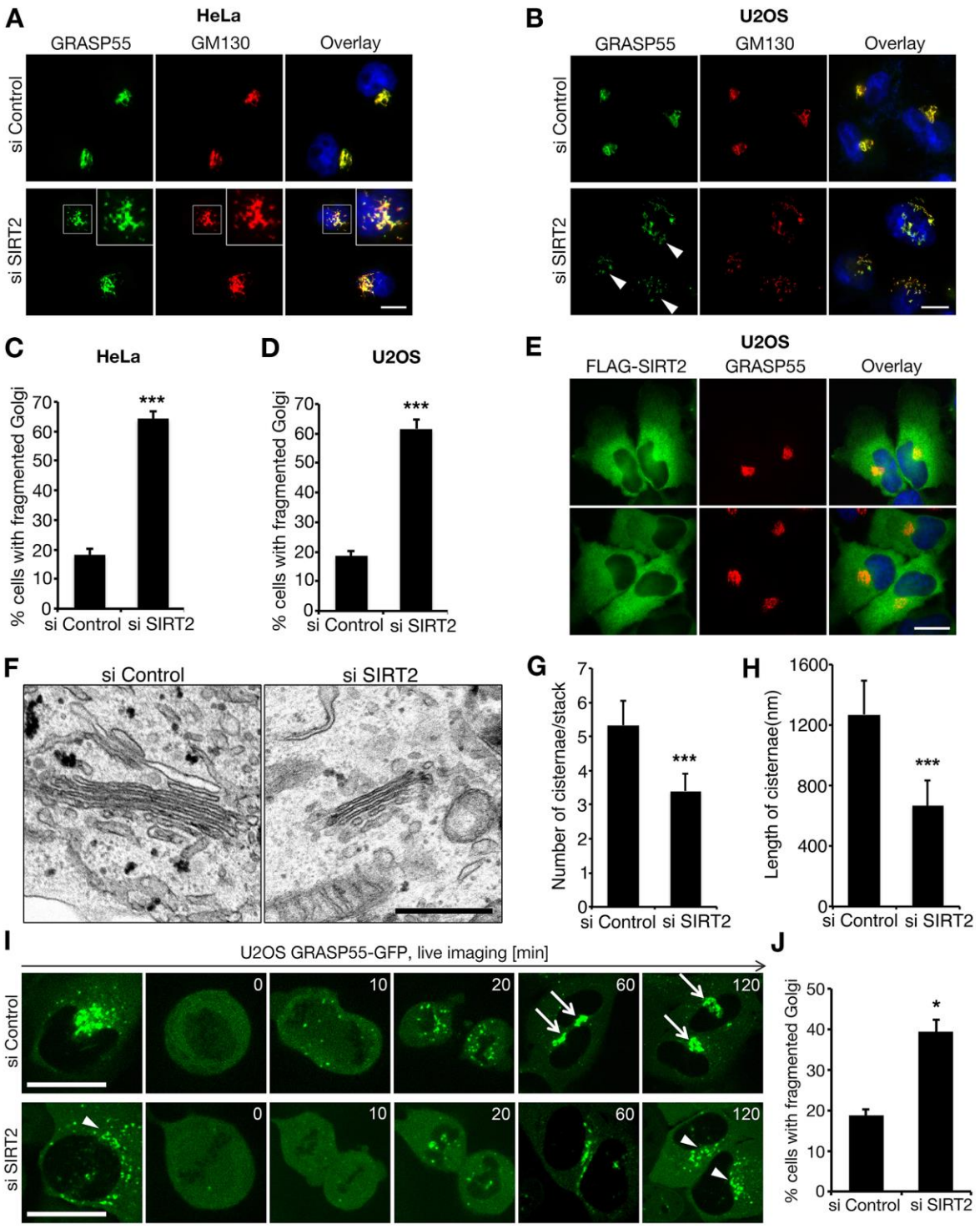


**Figure 2. SIRT2 depletion causes Golgi fragmentation and impairs Golgi structure formation.** **A-D.** Representative immunofluorescence images of HeLa (**A**) and U2OS (**B**) cells transfected with control or SIRT2 siRNA and co-stained for GRASP55 (green) and GM130 (red). Representative fragmented Golgi was enlarged in **A** as insets. Arrowheads in **B** indicate cells exhibiting fragmented Golgi. Scale bars: 20 μm. **C** and **D**. Quantification of Golgi fragmentation in **A** and **B** from three

independent experiments (n=210). **E.** SIRT2 overexpression does not significantly perturb the Golgi morphology in U2OS cells. Cells were transfected with FLAG-SIRT2 for 24 h and co-stained for FLAG (green) and GRASP55 (red). Two sets of cells are shown. Scale bar: 20 μm. **F.** HeLa cells were transfected with control or SIRT2 siRNA and analyzed by EM. Representative EM images are shown. Scale bar: 500 nm. **G.** Quantification of the number of cisternae per stack (n=20). **H.** Quantification of the length of Golgi cisternae (n=20). **I.** Live cell images of U2OS cells stably expressing GRASP55-GFP 72 h after SIRT2 siRNA transfection. Note that the Golgi is assembled in control cells (arrows) at 60 min but remains fragmented in SIRT2-depleted cells after 120 min (arrowheads). Scale bar: 20 μm. **J.** Quantification of Golgi fragmentation from **I** in control and SIRT2 knockdown cells using GRASP55-GFP as a marker (n=40). All quantification results in this figure are presented as mean ± SEM. Statistics was performed using two-tailed Student's t-test. *, $p < 0.05$; ***, $p < 0.001$.

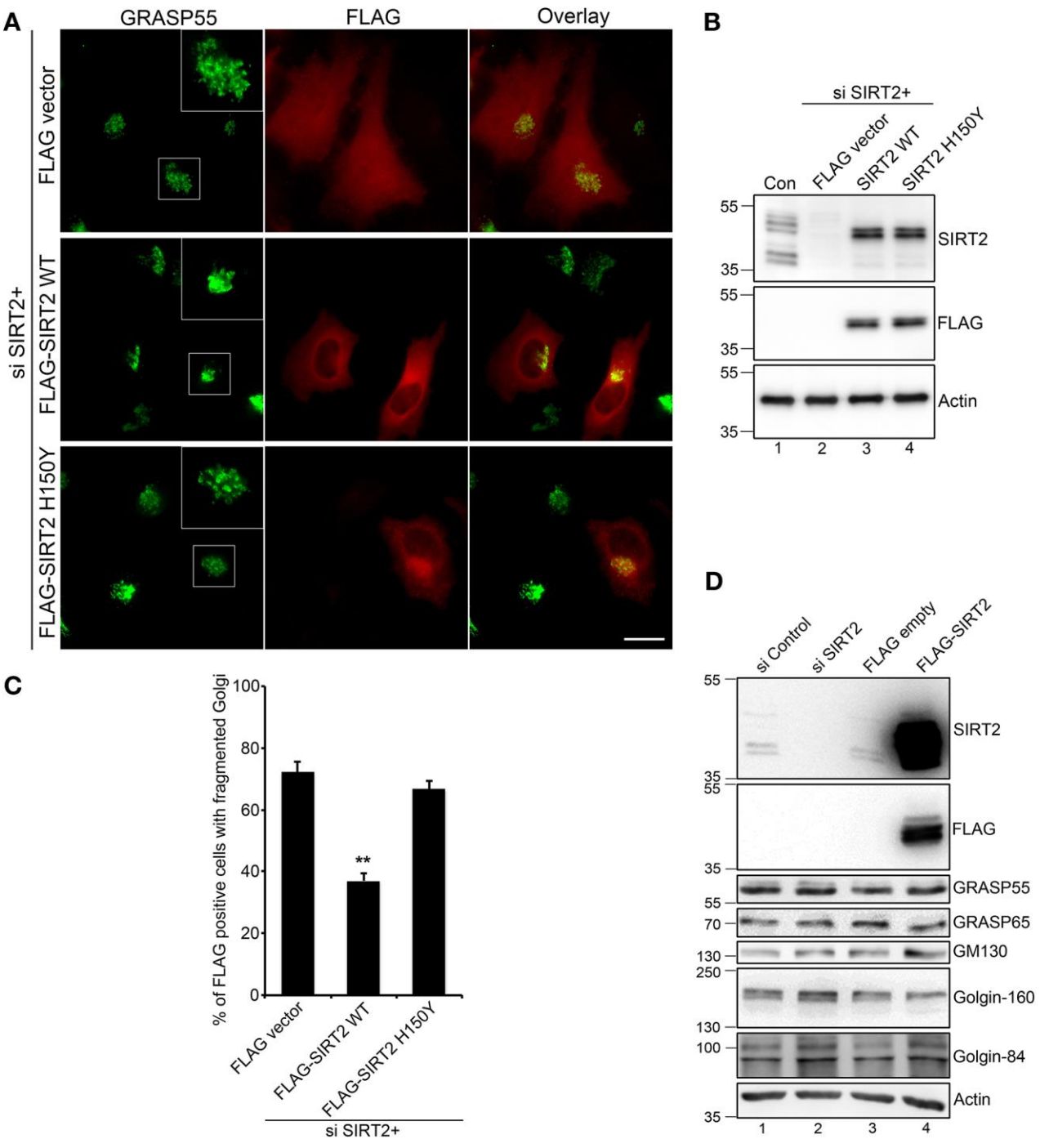


**Figure 3. The deacetylase activity of SIRT2 is required for maintaining an intact Golgi structure.** **A.** HeLa cells were transfected first with SIRT2 siRNA for 48 h, then with a FLAG vector (as control) or RNAi resistant FLAG-SIRT2 WT or H150Y mutant for another 24 h, and co-stained for GRASP55 (green) and FLAG (red). Scale bar: 20 μm. **B.** Cells in **A** were analyzed by Western blot to show the knockdown efficiency of endogenous SIRT2 and the expression level of FLAG-tagged SIRT2. **C.** Quantification of Golgi fragmentation in **A** from three independent experiments (n=200), and results

are presented as mean ± SEM. Statistics was performed using two-tailed Student's t-test. **, $p < 0.01$. **D.** HeLa cells were transfected with SIRT2 siRNA for 72 h or with FLAG-SIRT2 for 24 h, lysed, and blotted for indicated Golgi proteins. Control siRNA or an empty FLAG vector were used as controls.

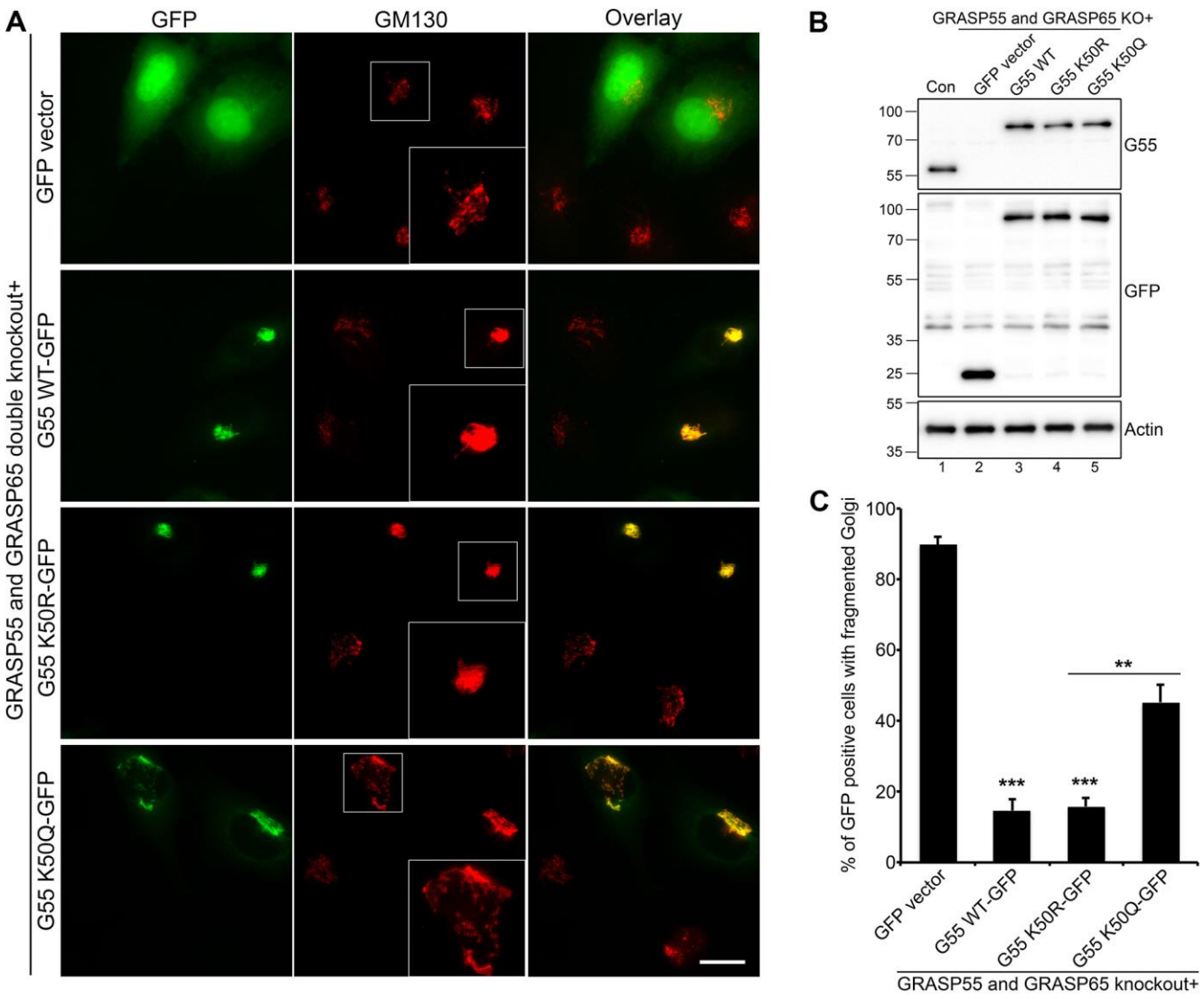


**Figure 4. GRASP55 deacetylation is required for Golgi structure formation.**

**A.** GRASP55/GRASP65 double knockout cells were transfected with a GFP vector (as control), GFP-tagged GRASP55 (G55 in the figure) WT, acetylation-deficient mutant K50R or acetylation-mimetic mutant K50Q for 24 h, and stained for GM130. Note that expression of WT and K50R efficiently rescued the Golgi structure. Scale bar: 20 μm. **B.** Cells in **A** were analyzed by Western blot to show the knockout efficiency of endogenous GRASP55 and the expression level of GFP-tagged GRASP55 WT and mutants. **C.** Quantification of Golgi fragmentation in **A** from three independent experiments (n=210). Quantification results are presented as mean ± SEM. Statistics was performed using two-tailed Student's t-test. **, $p < 0.01$; ***, $p < 0.001$.

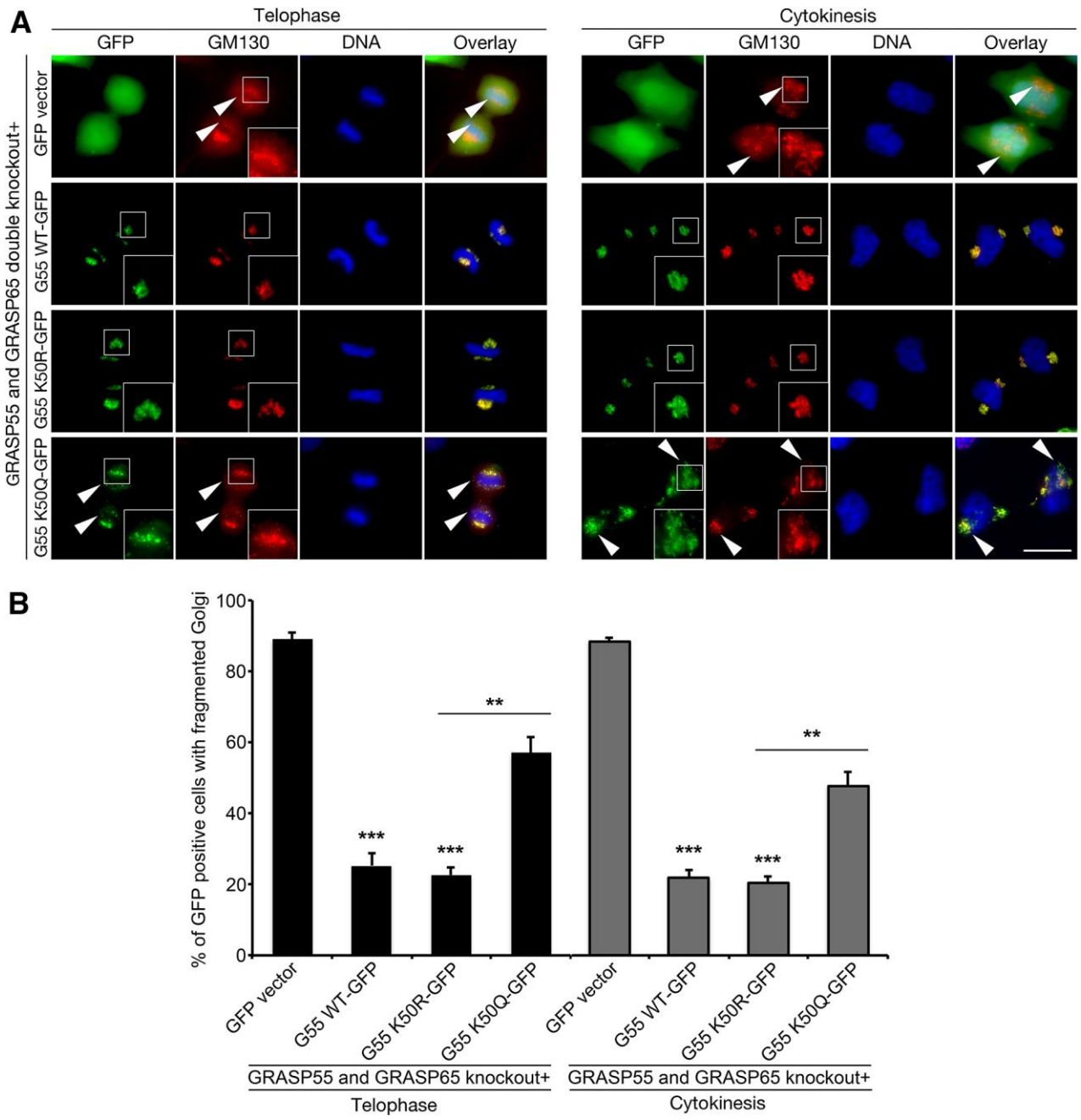


**Figure 5. GRASP55 deacetylation is required for Golgi reassembly at mitotic exit.**

**A.** GRASP55/GRASP65 double knockout cells were transfected with a GFP vector (as control), GFP-tagged GRASP55 WT, K50R or K50Q, and stained for GM130. Representative fluorescence images of telophase and cytokinesis cells are shown. Arrowheads indicate cells with fragmented Golgi. Representative Golgi morphology was enlarged as insets. Scale bar: 20 μm. **B.** Quantification of Golgi fragmentation in **A** from three independent experiments (n=200). Quantification results are presented as mean ± SEM. Statistics was performed using two-tailed Student's t-test. **, $p < 0.01$; ***, $p < 0.001$.

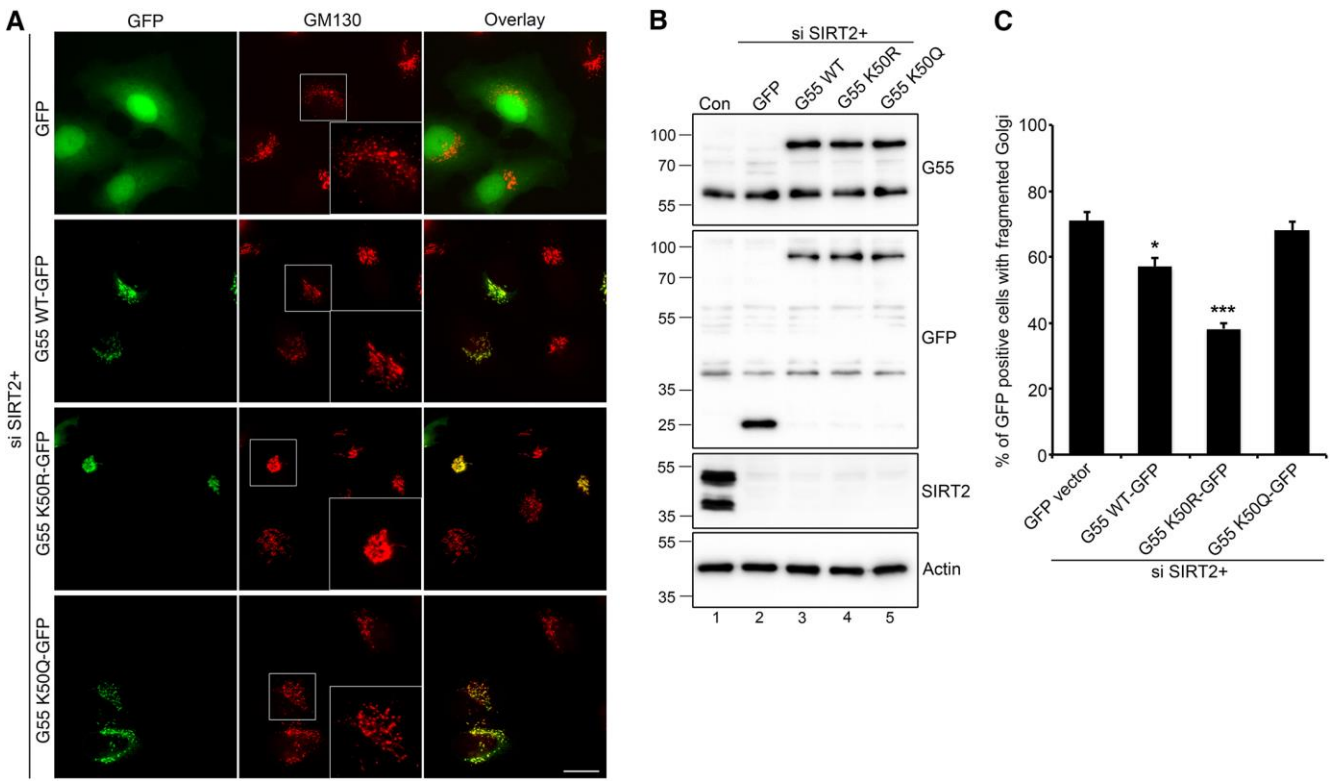


**Figure 6. Acetylation-deficient GRASP55 partially rescues Golgi fragmentation caused by SIRT2 depletion.**

**A.** HeLa cells were transfected first with SIRT2 siRNA for 48 h, then with a GFP vector (as control) or GFP-tagged GRASP55 WT, K50R or K50Q for another 24 h, and stained for GM130. Representative Golgi morphology was enlarged as insets. Arrowheads indicate Golgi fragments. Scale bar: 20 μm. **B.** Cells in **A** were analyzed by Western blot to show the knockdown efficiency of endogenous SIRT2 and the expression level of GFP-tagged GRASP55. **C.** Quantification of Golgi fragmentation in **A** from three independent experiments (n=221). Quantification results are presented as mean ± SEM. Statistics was performed using two-tailed Student's t-test. *, $p < 0.05$; ***, $p < 0.001$.

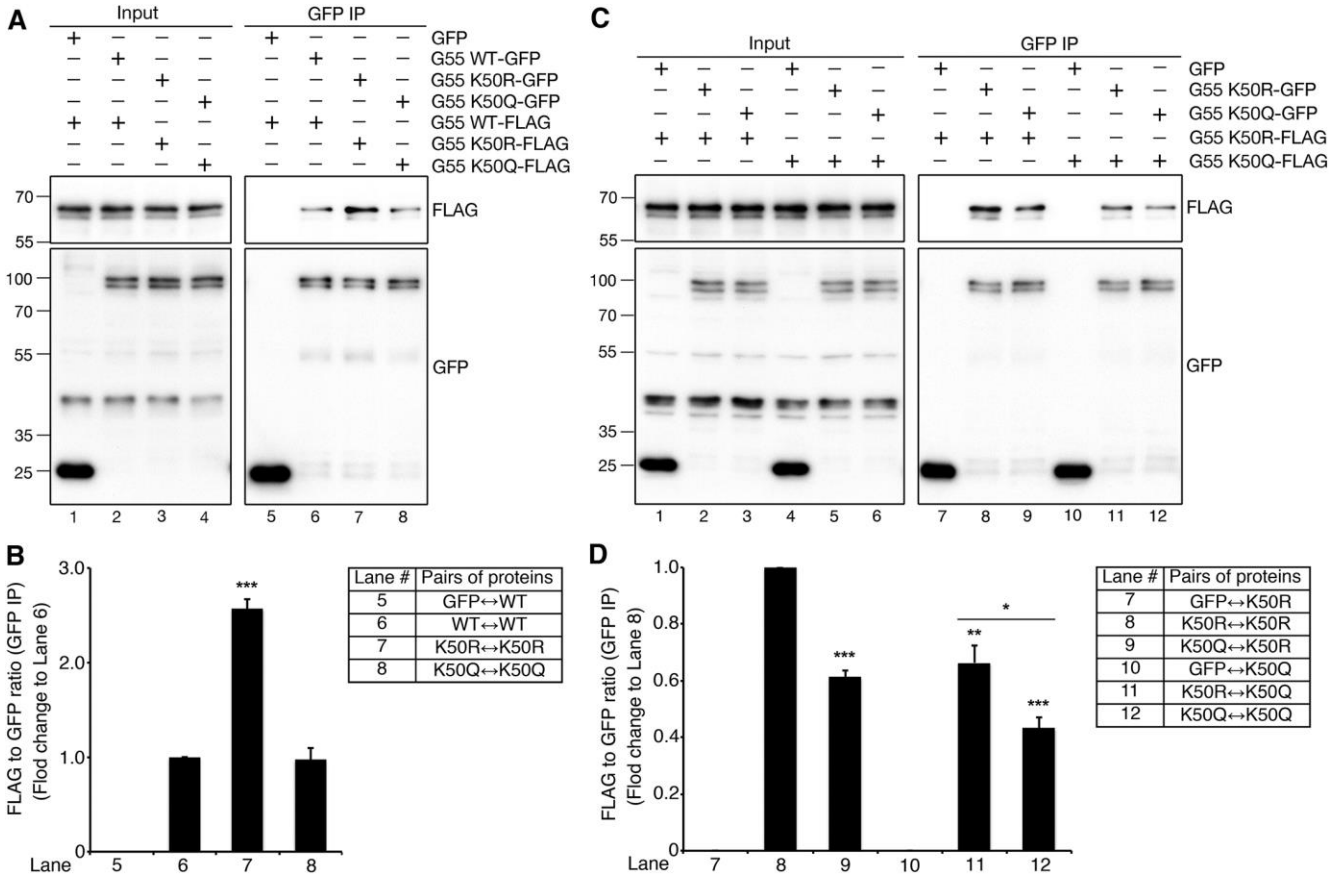


**Figure 7. GRASP55 deacetylation facilitates self-interaction.**

HeLa cells were co-transfected with GFP- and FLAG-tagged GRASP55 WT, K50R or K50Q constructs for 24 h and synchronized with nocodazole for another 18 h. Mitotic cells were collected, lysed, immunoprecipitated with a GFP antibody, and blotted for GFP and FLAG. **A-B**, Homologous GFP- and FLAG-tagged GRASP55 constructs were co-transfected, analyzed by co-immunoprecipitation, and quantified. **C-D**, Homologous or heterologous GFP- and FLAG-tagged GRASP55 constructs were co-transfected, analyzed, and quantified. **A, C.** Western blots of the co-immunoprecipitated proteins. **B, D.** Quantification of interaction efficiency in **A and C** by calculating the ratio of FLAG to GFP intensity in the GFP immunoprecipitates from three independent experiments. The homologous interaction of WT GRASP55 or the K50R mutant was normalized to 1 in **B** and **D**, respectively. Quantification results are presented as mean ± SEM. Statistics was performed using two-tailed Student's t-test. *, $p < 0.05$; **, $p<0.01$; ***, $p < 0.001$.

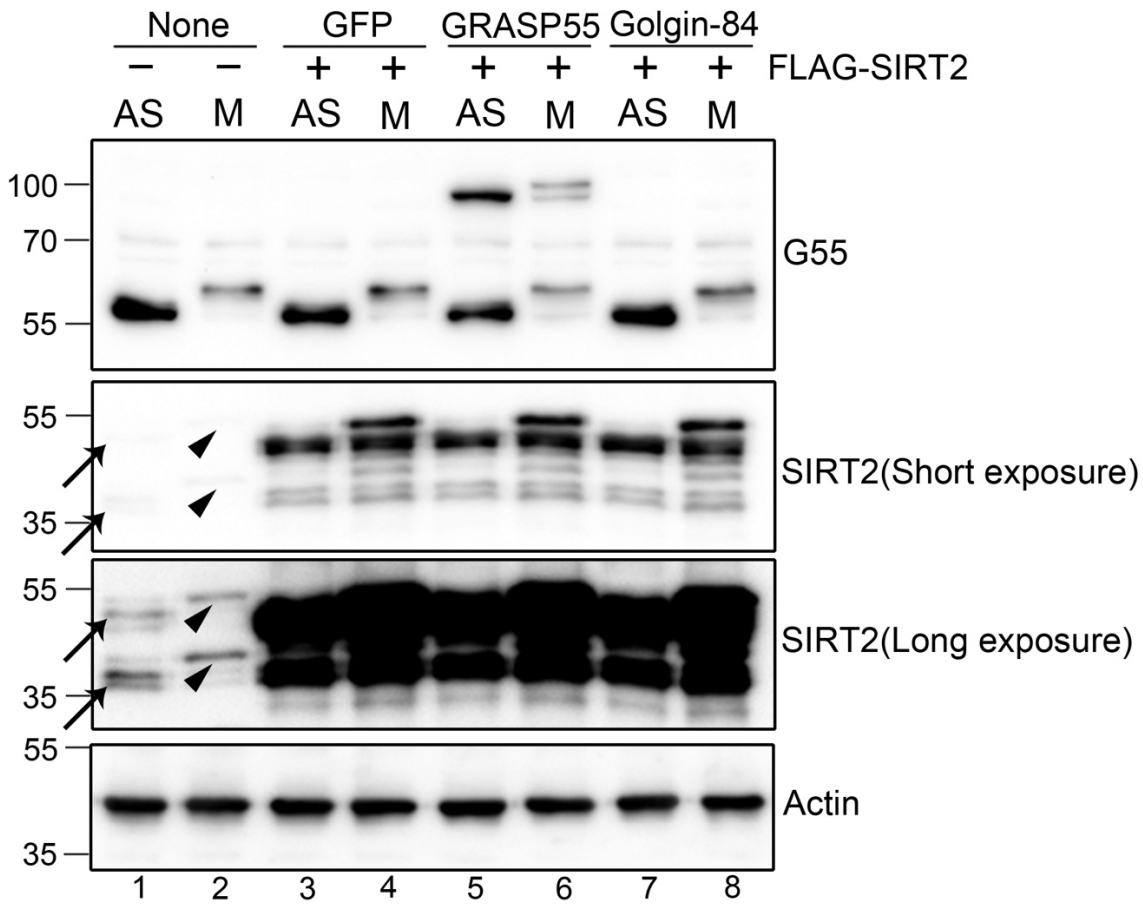


**Figure S1. The endogenous SIRT2 protein level is low.**
Asynchronous (AS) and mitotic HeLa cells or HeLa cells co-overexpressing GFP-tagged GRASP55 or Golgin-84 and FLAG-SIRT2 were lysed, blotted for GRASP55 (G55 in the figure) and SIRT2. Note that the endogenous SIRT2 level (lane 1 and 2) is very low compared to the overexpressed FLAG-SIRT2 (lane 3-8). Arrows indicate asynchronous SIRT2 bands, while arrowheads indicate mitotic SIRT2 bands.

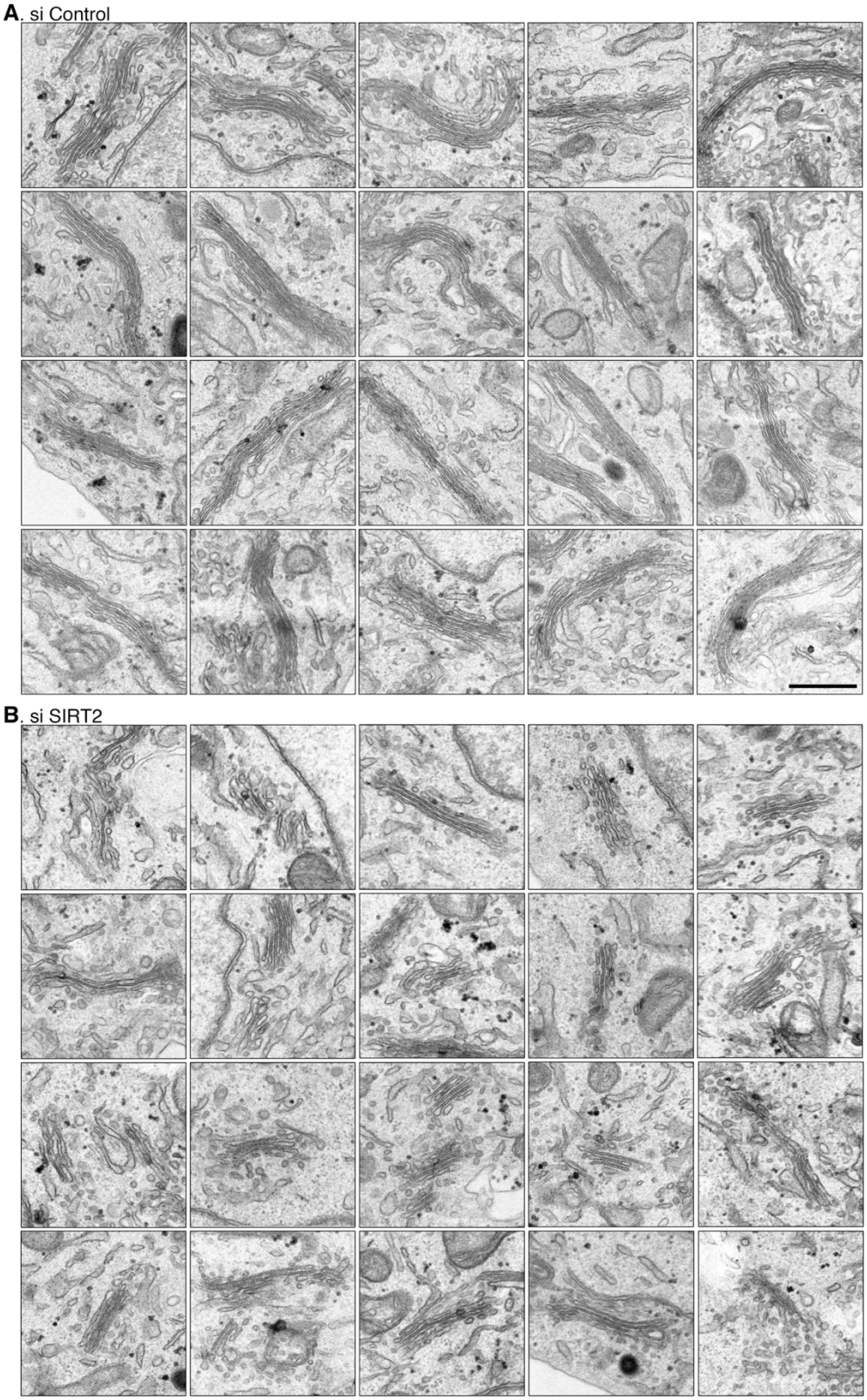


**Figure S2. SIRT2 is required for proper Golgi structure maintenance.**
HeLa cells were transfected with control (**A**) or SIRT2 (**B**) siRNA and analyzed by EM. Shown are galleries of EM images. The reduced average number or length of Golgi cisternae were frequently observed after SIRT2 depletion as displayed in **B**. Scale bar: 500 nm.

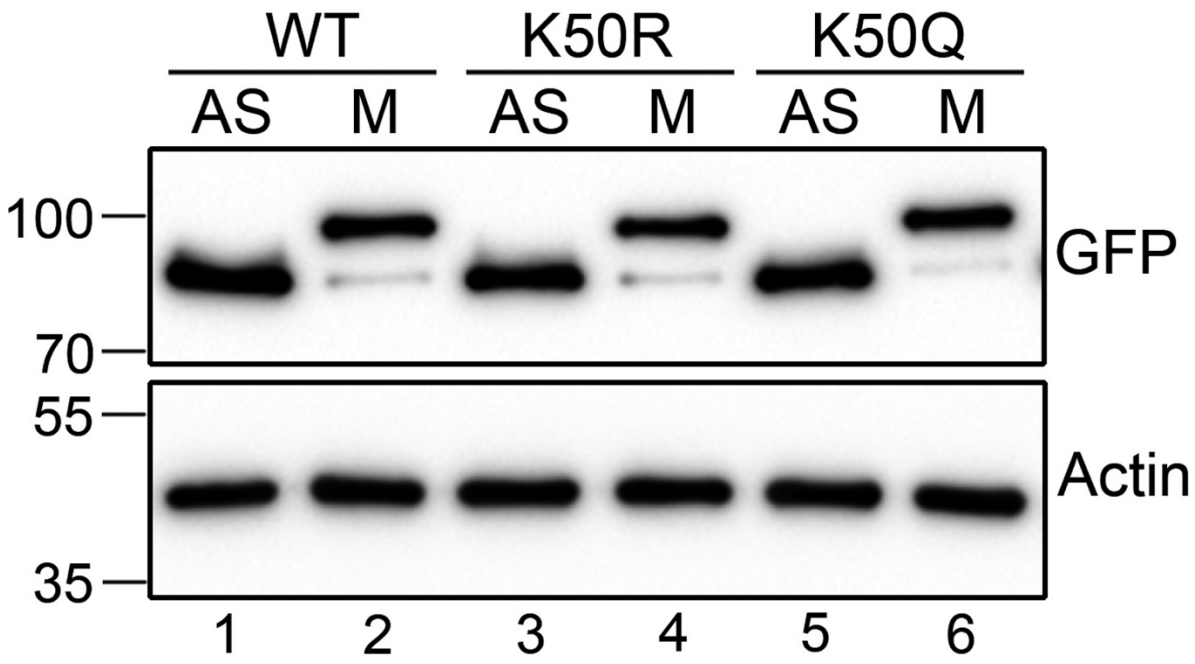


**Figure S3. GRASP55 acetylation status does not affect its phosphorylation in mitosis.**
HeLa cells were transfected with GFP-tagged GRASP55 WT, K50R or K50Q. Non-synchronized (AS) or mitotic (M) cells synchronized with nocodazole were lysed and blotted for GFP. Note that the GRASP55 phosphorylation status indicated by the band-shift is not affected by the acetylation mutations.

**Table S1.** Mass spectrometry analysis of GRASP55 post-translational modifications (acetylation, phosphorylation and ubiquitination) in asynchronous and mitotic HEK293T cells expressing GRASP55-GFP.

Click here to Download Table S1

**Table S2.** PRM (parallel reaction monitoring) mass spectrometry analysis of GRASP55-GFP K50 acetylation in mitotic HEK293T cells after silencing or overexpressing SIRT2.

Click here to Download Table S2

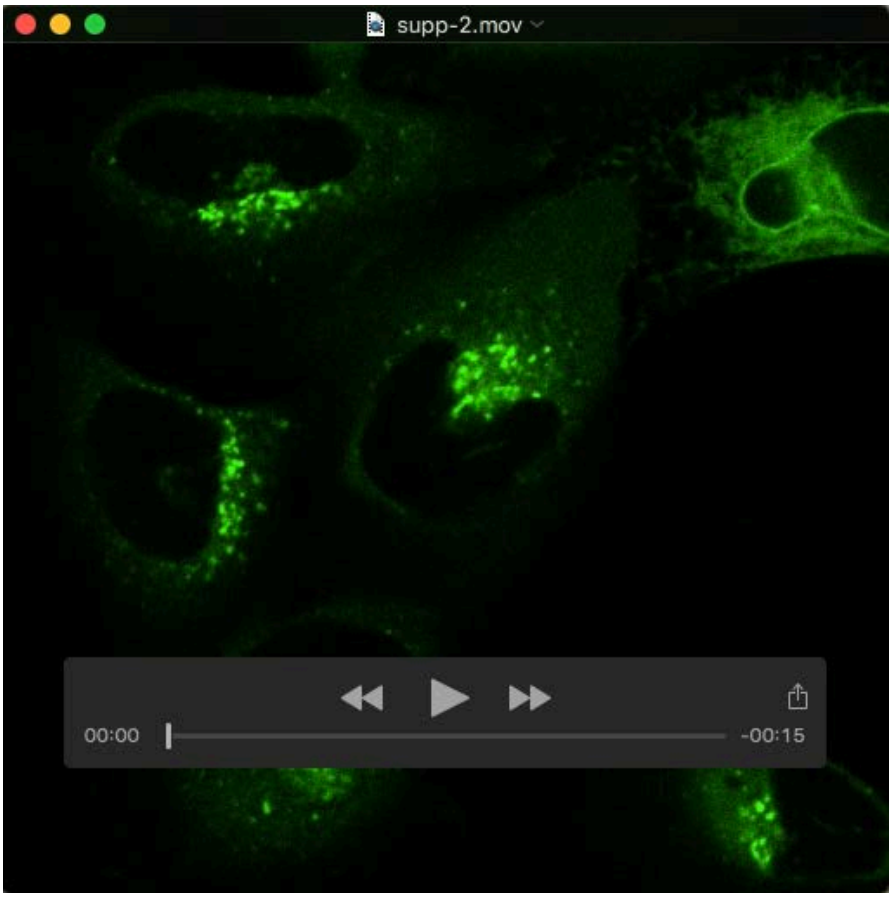


**Movie 1.** Live-cell imaging of GRASP55-GFP U2OS cells 72 h after transfection with si Control.

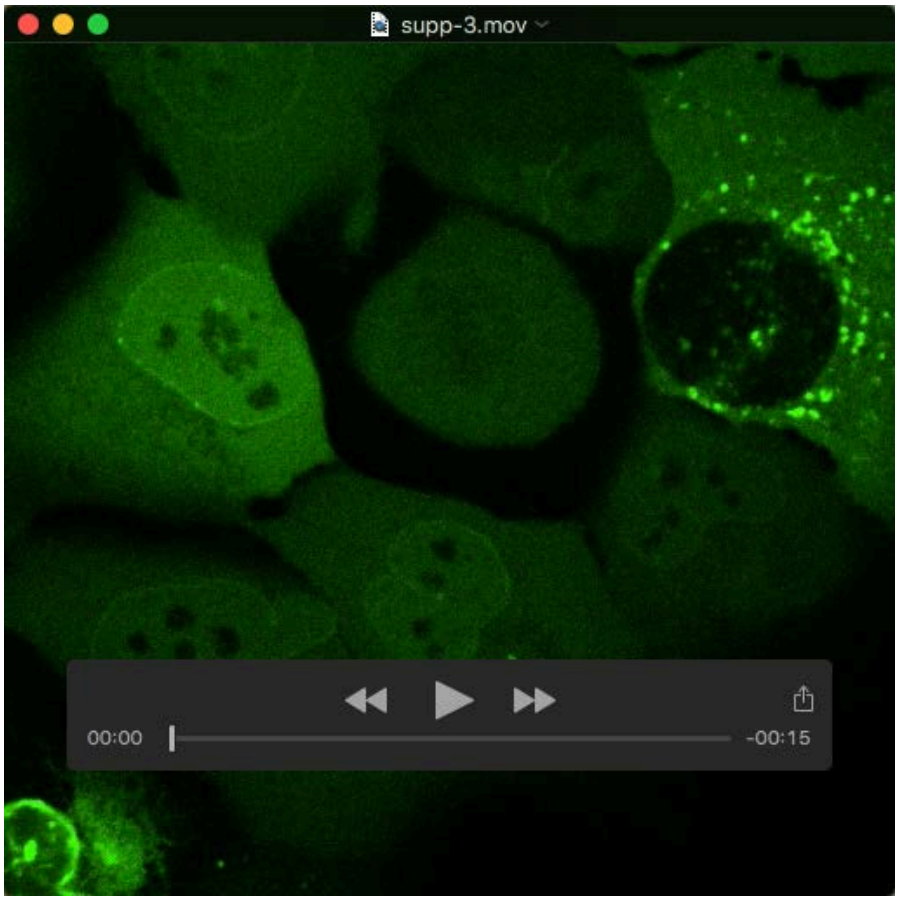


**Movie 2.** Live-cell imaging of GRASP55-GFP U2OS cells 72 h after transfection with si SIRT2.

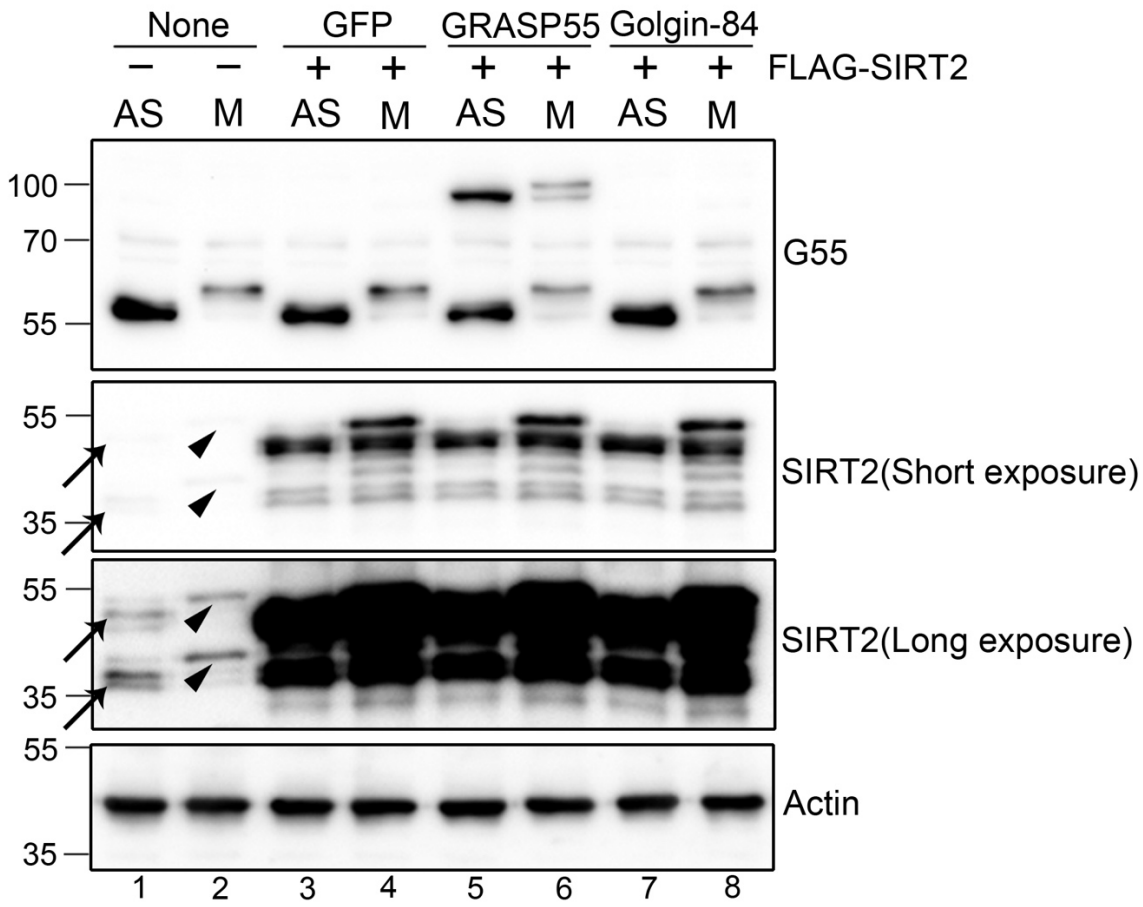


**Figure S1. The endogenous SIRT2 protein level is low.**
Asynchronous (AS) and mitotic HeLa cells or HeLa cells co-overexpressing GFP-tagged GRASP55 or Golgin-84 and FLAG-SIRT2 were lysed, blotted for GRASP55 (G55 in the figure) and SIRT2. Note that the endogenous SIRT2 level (lane 1 and 2) is very low compared to the overexpressed FLAG-SIRT2 (lane 3-8). Arrows indicate asynchronous SIRT2 bands, while arrowheads indicate mitotic SIRT2 bands.

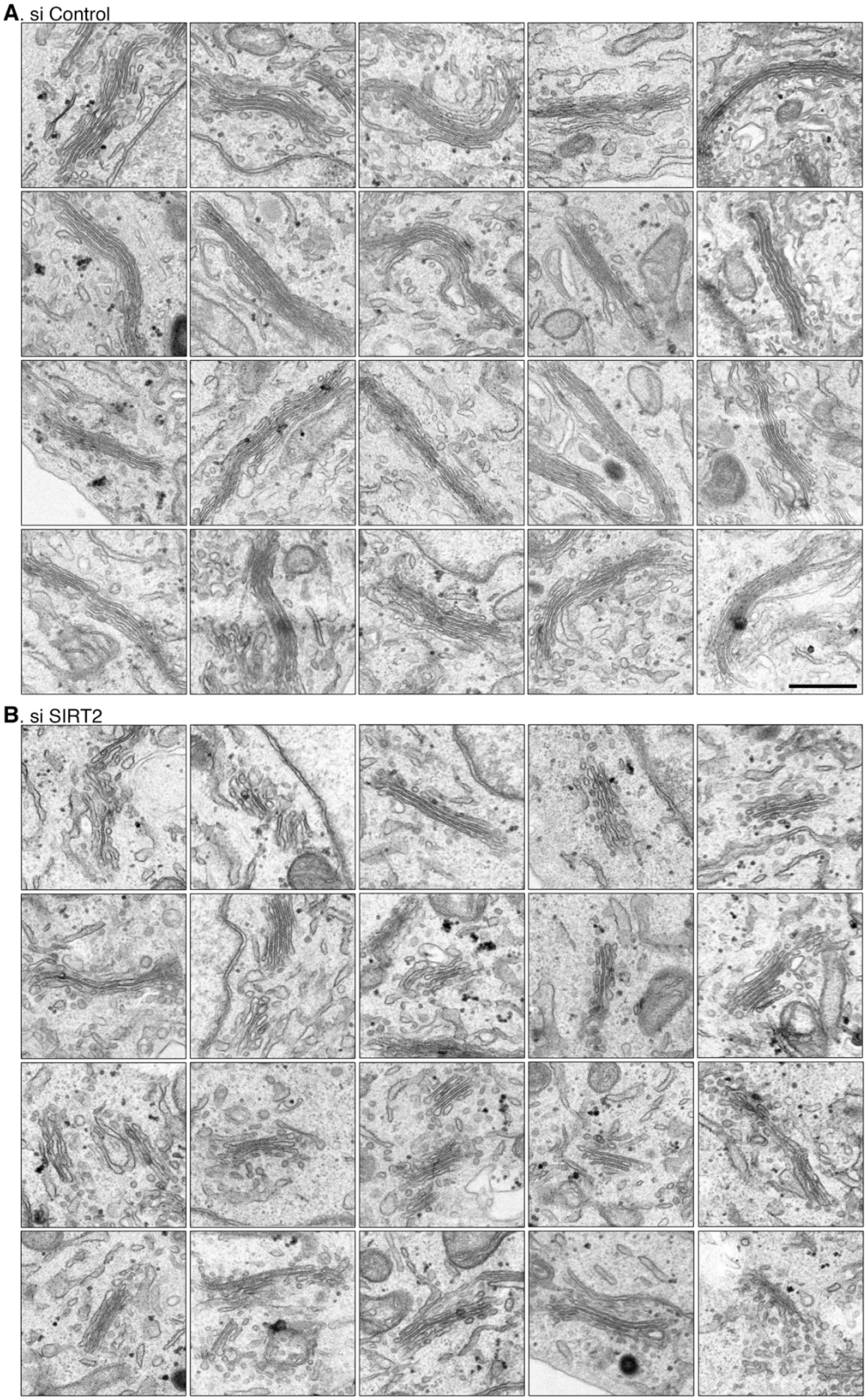


**Figure S2. SIRT2 is required for proper Golgi structure maintenance.**
HeLa cells were transfected with control (**A**) or SIRT2 (**B**) siRNA and analyzed by EM. Shown are galleries of EM images. The reduced average number or length of Golgi cisternae were frequently observed after SIRT2 depletion as displayed in **B**. Scale bar: 500 nm.

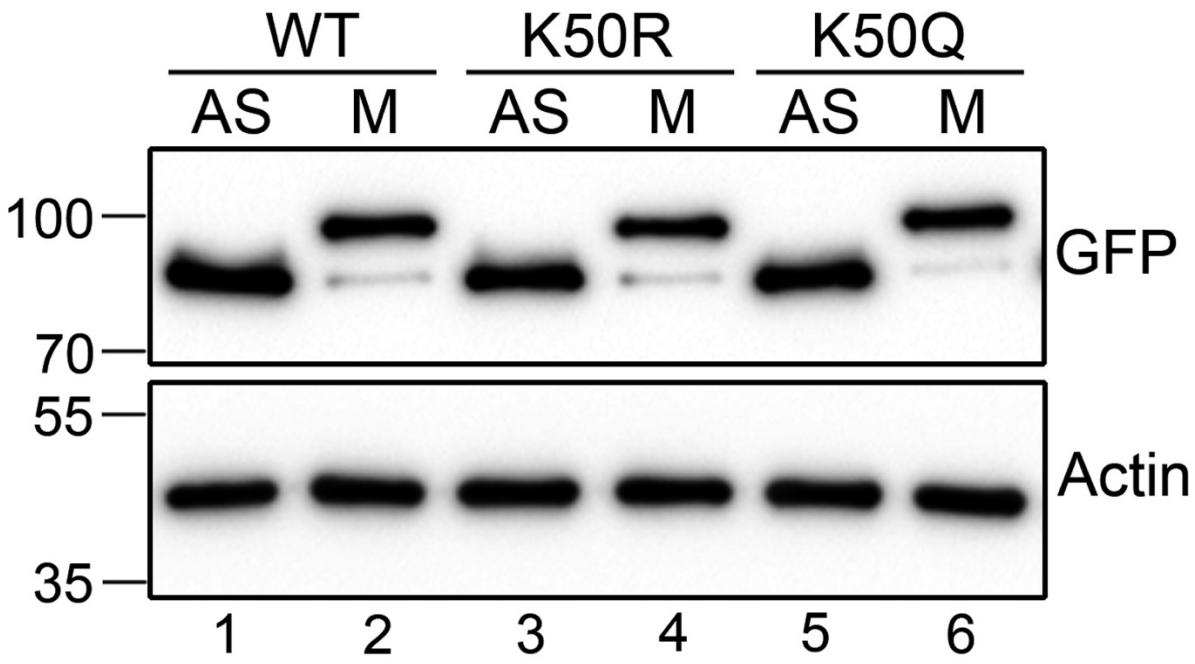


**Figure S3. GRASP55 acetylation status does not affect its phosphorylation in mitosis.**
HeLa cells were transfected with GFP-tagged GRASP55 WT, K50R or K50Q. Non-synchronized (AS) or mitotic (M) cells synchronized with nocodazole were lysed and blotted for GFP. Note that the GRASP55 phosphorylation status indicated by the band-shift is not affected by the acetylation mutations.

**Table S1.** Mass spectrometry analysis of GRASP55 post-translational modifications (acetylation, phosphorylation and ubiquitination) in asynchronous and mitotic HEK293T cells expressing GRASP55-GFP.

Click here to Download Table S1

**Table S2.** PRM (parallel reaction monitoring) mass spectrometry analysis of GRASP55-GFP K50 acetylation in mitotic HEK293T cells after silencing or overexpressing SIRT2.

Click here to Download Table S2

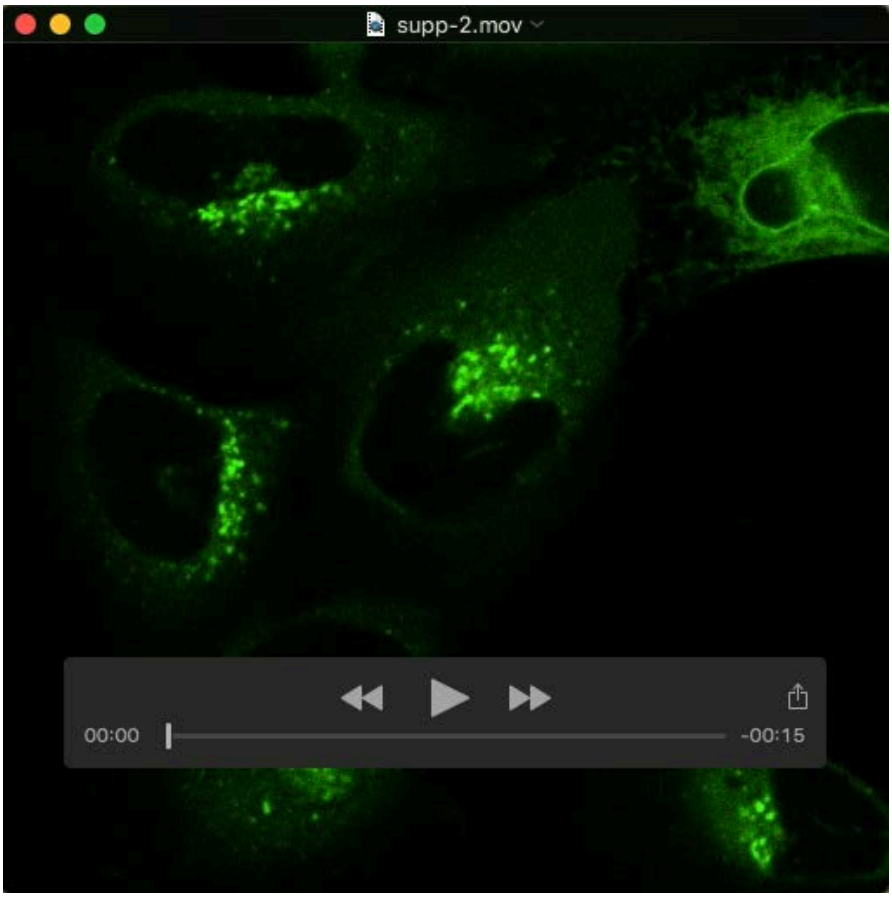


**Movie 1.** Live-cell imaging of GRASP55-GFP U2OS cells 72 h after transfection with si Control.

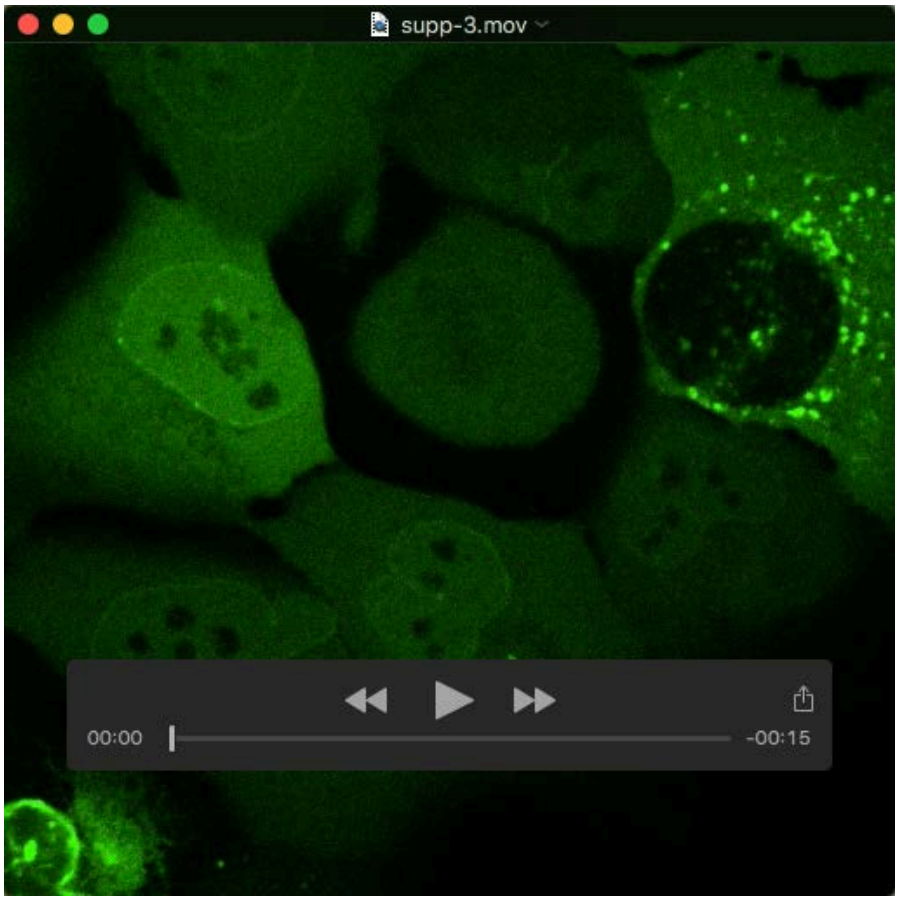


**Movie 2.** Live-cell imaging of GRASP55-GFP U2OS cells 72 h after transfection with si SIRT2.